

Nonsubsampled Graph Filter Banks and Distributed Implementation

Junzheng Jiang, Cheng Cheng, and Qiyu Sun

Abstract

In this paper, we consider nonsubsampled graph filter banks (NSGFBs) to process data on a graph in a distributed manner. Given an analysis filter bank with small bandwidth, we propose algebraic and optimization methods of constructing synthesis filter banks such that the corresponding NSGFBs provide a perfect signal reconstruction in the noiseless setting. Moreover, we prove that the proposed NSGFBs can control the resonance effect in the presence of bounded noise and they can limit the influence of shot noise primarily to a small neighborhood of its location on the graph. For an NSGFB on a graph of large size, a distributed implementation has a significant advantage, since data processing and communication demands for the agent at each vertex depend mainly on its neighboring topology. In this paper, we propose an iterative distributed algorithm to implement the proposed NSGFBs. Based on NSGFBs, we also develop a distributed denoising technique which is demonstrated to have satisfactory performance on noise suppression.

Keywords: Graph signal processing, Graph filter bank, Distributed algorithm, Noise suppression, Random geometric graph, Laplacian matrix.

I. Introduction

Spatially distributed networks (SDNs) have an agent at each location equipped with some data processing and communication abilities, and they have been widely used in wireless sensor networks, power grids and many real world applications ([1]–[5]). Data collected by an SDN resides naturally on vertices of a graph. Graph signal processing provides an innovative framework to process data on graphs. Many concepts, such as the Fourier transform, wavelet transform and filter banks, in classical signal processing, have been extended to graph settings in recent years. However there are still lots of fundamental problems unexplored or not completely answered ([6]–[11]).

The wavelet transform is one of the most prominent techniques to process signals in regular domains ([12]–[14]). During the past decades, graph wavelet transforms have been introduced and some of them are designed using the eigenvalue and eigenspace information of the graph Laplacian matrix ([15]–[19]). Graph wavelet transform is under the same theoretical structure with graph filter banks and the corresponding wavelet filter bank carries a down and up-sampling procedure ([7], [8], [20]–[27]). Several forms of the down and up-sampling procedure have been defined by the partitioned graph coloring in [20], the maximum spanning tree structure of the graph in [25], and the SVD decomposition of the graph Laplacian matrix in [26]. A proper definition of the down and up-sampling procedure is not obvious especially when the residing graph is of large size and complicated topological structure. This motivates us to consider a *nonsubsampled graph filter bank* (NSGFB) that contains an analysis filter bank $(\mathbf{H}_0, \mathbf{H}_1)$ and a synthesis filter bank $(\mathbf{G}_0, \mathbf{G}_1)$, see Figure 1 for its block diagram. The analysis filter bank decomposes a graph signal into two components carrying different frequency information. The nonsubsampled structure in an NSGFB greatly simplifies the design of analysis filter banks for spectral decomposition and synthesis filter banks for signal reconstruction.

Jiang is with the School of Information and Communication, Guilin University of Electronic Technology, Guilin 541004, China; Cheng is with the Department of Mathematics, Duke University, and Statistical and Applied Mathematical Sciences Institute (SAMSI), Durham, NC 27708; and Sun is with the Department of Mathematics, University of Central Florida, Orlando, Florida 32816. Emails: jzjiang@guet.edu.cn; cheng87@math.duke.edu; qiyu.sun@ucf.edu. This work is partially supported by the National Natural Science Foundation of China (Grant No. 61761011), SAMSI under the National Science Foundation (DMS-1638521), and the National Science Foundation (DMS-1412413).

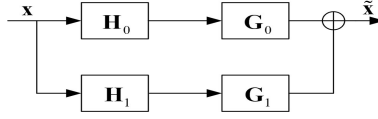


Fig. 1. Block diagram of an NSGFB with analysis filter bank $(\mathbf{H}_0, \mathbf{H}_1)$ and synthesis filter bank $(\mathbf{G}_0, \mathbf{G}_1)$, where \mathbf{x} is the input of the NSGFB and $\tilde{\mathbf{x}}$ is its output.

Filter banks can be implemented either in a centralized system or a cooperative decentralized (distributed) system. In a centralized system, a central facility receives data from agents at vertices, performs designed data processing and sends the processed data back to agents at vertices. In a decentralized system, the agent at each vertex has certain data processing ability to perform designed data processing, and data collected from an agent at each vertex is shared only with neighboring vertices. Most filter banks on graphs are designed for centralized processing, however for the implementation of filter banks on a graph of large size, a centralized system may suffer from high computational burden and call for significant efforts to create a data exchange network. For signal processing on an SDN or a graph of large size, a distributed implementation provides an indispensable tool. It has been used for signal sampling and reconstruction on an SDN in [5], graph signal inpainting in [28] and economic dispatch in power networks [29]. The reader may refer to [5], [28]–[34] and references therein on distributed implementation of signal processing on graphs. In a distributed implementation of the analysis and synthesis procedures of an NSGFB, signal information on each vertex is transmitted only to neighboring vertices, which dramatically reduces the computational cost and calls for low energy consumption. In this paper, we study NSGFBs on a cooperative decentralized system from design to distributed implementation, and then to distributed signal denoising.

A. Main contributions

An important concept for an NSGFB is the *perfect reconstruction* condition, i.e., the output $\tilde{\mathbf{x}}$ in Figure 1 is always the same as the input \mathbf{x} , which can be characterized by the following matrix equation,

$$\mathbf{G}_0\mathbf{H}_0 + \mathbf{G}_1\mathbf{H}_1 = \mathbf{I}, \quad (\text{I.1})$$

where $(\mathbf{H}_0, \mathbf{H}_1)$ and $(\mathbf{G}_0, \mathbf{G}_1)$ are its analysis and synthesis filter bank respectively. Given an analysis filter bank, the existence of synthesis filter banks is theoretically guaranteed so that the corresponding NSGFB satisfies the perfect reconstruction condition (I.1) ([13], [14]). The first contribution of this paper is that we introduce two methods to construct localized synthesis filter banks. In the first approach, the synthesis filter bank is obtained by solving a Bezout identity for polynomials. Its bandwidth could be no larger than the bandwidth of the analysis filter bank. In the second approach, the synthesis filter bank is the solution of a constrained optimization problem. It does not necessarily have small bandwidth, however it has an exponential off-diagonal decay. Consequently, the output of the corresponding localized NSGFB suffers primarily in a small neighborhood of vertices where agents lose data processing ability and/or communication capability.

In some real world applications of an NSGFB, the input \mathbf{x} is the original signal \mathbf{x}_o corrupted by an additive noise ϵ . In addition, the subband signals $\mathbf{z}_0 = \mathbf{H}_0\mathbf{x}$ and $\mathbf{z}_1 = \mathbf{H}_1\mathbf{x}$ are usually processed via some (non)linear procedure, such as hard/soft thresholding and quantization. Then the output

$$\tilde{\mathbf{x}} = \mathbf{G}_0\Psi_0(\mathbf{H}_0(\mathbf{x}_o + \epsilon)) + \mathbf{G}_1\Psi_1(\mathbf{H}_1(\mathbf{x}_o + \epsilon)) \quad (\text{I.2})$$

of the NSGFB is no longer the original signal \mathbf{x}_o , where ϵ is the input noise, and Ψ_0, Ψ_1 are subband processing operators. The robustness of an NSGFB is of paramount importance. For an SDN, an agent at each vertex operates almost independently and the noise that arises at each vertex of the graph is usually contained in some range [5]. So we may use a bounded deterministic/random noise model for NSGFBs on a distributed system. A reasonable fidelity measure to assess the robustness of an NSGFB is the bounded

difference $\|\tilde{\mathbf{x}} - \mathbf{x}_o\|_\infty$, instead of the conventional least squares error $\|\tilde{\mathbf{x}} - \mathbf{x}_o\|_2$, between the original signal \mathbf{x}_o and the output signal $\tilde{\mathbf{x}}$ ([5], [35], [36]). Here for $1 \leq p \leq \infty$, ℓ^p is the space of all p -summable sequences with norm $\|\cdot\|_p$. The second contribution of this paper is that for the NSGFB with analysis filter bank having small bandwidth and synthesis filter banks obtained from our approaches, we establish a quantitative estimate on the bounded difference $\|\tilde{\mathbf{x}} - \mathbf{x}_o\|_\infty$, which is independent on the size of the graph \mathcal{G} . This indicates that the proposed NSGFB can control the resonance effect in the presence of bounded additive noises.

For an NSGFB on a graph of large size, a distributed implementation may provide an indispensable tool. The third contribution of this paper is that we propose an iterative distributed algorithm to implement the synthesis procedure of an NSGFB rather than finding the synthesis filter bank explicitly. The keys behind the algorithm are the decomposition (II.1) that splits the whole residing graph into a family of overlapping subgraphs of appropriate size, and an observation that solutions of some global optimization problem can be locally approximated by solutions of local optimization problems, when the objective function and constraints are well localized [5]. As an application of NSGFBs, we develop a distributed denoising technique that has satisfactory performance on noise suppression.

B. Organization

In Section II, we briefly review some fundamental concepts of graphs and introduce an overlapping graph decomposition (II.1). In Section III, we introduce the concept of graph filters on ℓ^p , $1 \leq p \leq \infty$, and show that bounded filters with finite bandwidth are graph filters on ℓ^p , see Definition III.1 and Proposition III.3. In Section IV, we discuss the analysis filter bank $(\mathbf{H}_0, \mathbf{H}_1)$ of an NSGFB which are required to have small bandwidth, to pass/block the normalized constant signal, and to have stability on ℓ^2 , see Assumptions IV.1, IV.2 and IV.4. We show that analysis filter banks have stability on ℓ^p for all $1 \leq p \leq \infty$, with an estimate on their lower and upper ℓ^p -stability bounds independent on the size of the graph, see Theorem IV.6. In Section V, we propose an algebraic design of synthesis filter banks $(\mathbf{G}_0, \mathbf{G}_1)$ when analysis filters \mathbf{H}_0 and \mathbf{H}_1 are polynomials of the symmetric normalized Laplacian on the graph, see Theorem V.1. In Section VI, we consider the construction of synthesis filter banks $(\mathbf{G}_0, \mathbf{G}_1)$ by solving the constrained optimization problem (VI.1) and (VI.2) with the objective function consisting of Frobenius norms of \mathbf{G}_0 and \mathbf{G}_1 , see (VI.4) and Theorem VI.1. In Section VII, we propose an exponentially convergent iterative algorithm (VII.9) and (VII.10) to implement the synthesis procedure, where each iteration can be implemented in a distributed manner, see Theorem VII.2 and Algorithm VII.1. In Section VIII, we create a distributed denoising technique associated with spline NSGFBs, see Figure 5, and demonstrate its performance for signal denoising on graphs of large size. All proofs are collected in the appendices.

C. Notation

We use the common convention of representing matrices and vectors with bold letters and scalars with normal letters. For a matrix \mathbf{A} , denote its transpose, trace, Frobenius norm and operator norm on ℓ^p , $1 \leq p \leq \infty$, by \mathbf{A}^T , $\text{tr}(\mathbf{A})$, $\|\mathbf{A}\|_F$ and $\|\mathbf{A}\|_{\mathcal{B}_p}$ respectively. For a graph \mathcal{G} , denote its adjacency matrix and degree matrix by $\mathbf{A}_{\mathcal{G}}$ and $\mathbf{D}_{\mathcal{G}}$ respectively, and define its Laplacian matrix by $\mathbf{L}_{\mathcal{G}} := \mathbf{D}_{\mathcal{G}} - \mathbf{A}_{\mathcal{G}}$ and its symmetric normalized Laplacian matrix by $\mathbf{L}_{\mathcal{G}}^{\text{sym}} := \mathbf{D}_{\mathcal{G}}^{-1/2} \mathbf{L}_{\mathcal{G}} \mathbf{D}_{\mathcal{G}}^{-1/2}$. For a scalar t , let $\text{sgn}(t)$, $[t]$ and t_+ be its sign, integral part and positive part respectively, and \mathbf{t} be the vector of appropriate size with all entries taking value t . For a set F , denote its cardinality and indicator function by $\#F$ and χ_F respectively.

II. PRELIMINARIES ON GRAPHS

Let $\mathcal{G} := (V, E)$ be a graph, where $V = \{1, 2, \dots, N\}$ is the set of vertices and E is the set of edges ([5], [6]). For the distributed implementation of an NSGFB, we require that the residing graph \mathcal{G} has certain global features.

Assumption II.1. Throughout the paper, we consider simple graphs \mathcal{G} , i.e., they are undirected and unweighted, and they do not contain self-loops and multiple edges.

Take $r \geq 0$. For a graph $\mathcal{G} = (V, E)$ satisfying Assumption II.1, we define the r -neighborhood and the r -neighboring subgraph of $i \in V$ by $B(i, r) := \{j \in V : \rho(i, j) \leq r\}$ and $\mathcal{G}_{i,r} := (B(i, r), E(i, r))$ respectively, where $E(i, r)$ contains all edges of the graph \mathcal{G} with endpoints in $B(i, r)$, and $\rho(i, j)$ is the geodesic distance between vertices i and j in V . Then for $r \geq 1$, we can decompose the graph \mathcal{G} into a family of overlapping subgraphs $\mathcal{G}_{i,r}, i \in V$, of diameters at most $2r$,

$$\mathcal{G} = \cup_{i \in V} \mathcal{G}_{i,r}. \quad (\text{II.1})$$

For distributed implementation for an NSGFB, we presume that numbers of vertices in the r -neighborhood of any vertex are dominated by a polynomial about r .

Assumption II.2. Throughout the paper, we consider graphs \mathcal{G} with the counting measure μ having polynomial growth, i.e., there exist positive constants $D_1(\mathcal{G})$ and d such that

$$\mu(B(i, r)) \leq D_1(\mathcal{G})(r + 1)^d \quad (\text{II.2})$$

for all $i \in V$ and $r \geq 0$, where $\mu(F) := \#F$ for all $F \subset V$.

The minimal constants d and $D_1(\mathcal{G})$ in (II.2) are called as *Beurling dimension* and *density* of the graph \mathcal{G} respectively [5].

The decomposition (II.1) plays a crucial role in the proposed distributed implementation for an NSGFB, and the selection of the radius parameter r in (II.1) depends on Beurling dimension d and density $D_1(\mathcal{G})$ of the graph \mathcal{G} , see Theorem VII.2. Accordingly, we expect that the Beurling dimension d and density $D_1(\mathcal{G})$ of the graph \mathcal{G} are much smaller than (or even independent on) the size of the graph, which implies that the graph \mathcal{G} should be sparse. Shown in Figure 2 are two representative graphs that satisfy Assumptions II.1 and II.2:

- The Minnesota traffic graph with 2642 vertices, where each vertex represents a spatial location in the state of Minnesota equipped with a traffic monitoring sensor and each edge denotes a direct communication link between monitoring sensors ([20], [21]).
- The random geometric graph RGG_N with N vertices randomly deployed in the region $[0, 1]^2$ and an edge existing between two vertices if their physical distance is not larger than $\sqrt{2}N^{-1/2}$ ([26], [37], [38]).

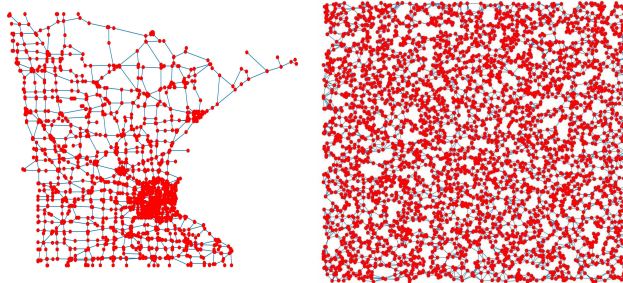


Fig. 2. Plotted on the left is the Minnesota traffic graph that has Beurling dimension 2 and density 2.1378. On the right is a random geometric graph with $N = 4096$, which has Beurling dimension 2 and density 3.0775.

III. GRAPH SIGNAL AND FILTERING

Let $\mathcal{G} = (V, E)$ satisfy Assumptions II.1 and II.2. A *signal* \mathbf{x} residing on the graph \mathcal{G} is a vector $(x_i)_{i \in V}$, where x_i refers to the signal value at vertex $i \in V$. In SDNs and many real world applications, data collected belongs to some sequence space ℓ^p , $1 \leq p \leq \infty$ ([5], [35], [36]).

A *filter* \mathbf{A} on the graph \mathcal{G} is a linear transformation from one signal \mathbf{x} on \mathcal{G} to another signal $\mathbf{y} = \mathbf{A}\mathbf{x}$ on \mathcal{G} , which is usually represented by a matrix $\mathbf{A} = (a(i, j))_{i, j \in V}$. A filter \mathbf{A} is expected to map a signal with finite energy to another signal with finite energy and a bounded signal to another bounded signal. A quantitative description of the above filtering procedure is

$$\|\mathbf{A}\mathbf{x}\|_p \leq C\|\mathbf{x}\|_p \text{ for all } \mathbf{x} \in \ell^p, \quad (\text{III.1})$$

where $1 \leq p \leq \infty$ and C is a positive constant.

Definition III.1. Let $1 \leq p \leq \infty$. We say that \mathbf{A} is a *graph filter on ℓ^p* if (III.1) is satisfied, and we call the minimal constant C for (III.1) to hold, denoted by $\|\mathbf{A}\|_{\mathcal{B}_p}$, the *filter bound on ℓ^p* .

In some practical applications ([8], [20], [21], [22], [26], [39]), a graph filter \mathbf{A} is a polynomial $P(t) := \sum_{l=0}^L p_l t^l$ of the symmetric normalized Laplacian $\mathbf{L}_{\mathcal{G}}^{\text{sym}}$ on \mathcal{G} , i.e.,

$$\mathbf{A} = P(\mathbf{L}_{\mathcal{G}}^{\text{sym}}) = p_0 \mathbf{I} + \sum_{l=1}^L p_l (\mathbf{L}_{\mathcal{G}}^{\text{sym}})^l. \quad (\text{III.2})$$

Let $0 \leq \lambda_1 \leq \lambda_2 \leq \dots \leq \lambda_N \leq 2$ be eigenvalues of the symmetric normalized Laplacian $\mathbf{L}_{\mathcal{G}}^{\text{sym}}$ and write

$$\mathbf{L}_{\mathcal{G}}^{\text{sym}} = \mathbf{U}^T \mathbf{\Lambda} \mathbf{U}, \quad (\text{III.3})$$

where $\mathbf{U}^T = [\mathbf{u}_1, \dots, \mathbf{u}_N]$ is an orthogonal matrix and $\mathbf{\Lambda} = \text{diag}(\lambda_1, \dots, \lambda_N)$ is a diagonal matrix. Then

$$\mathbf{A} = \mathbf{U}^T P(\mathbf{\Lambda}) \mathbf{U}, \quad (\text{III.4})$$

and the filter bound $\|\mathbf{A}\|_{\mathcal{B}_2}$ can be evaluated explicitly,

$$\|\mathbf{A}\|_{\mathcal{B}_2} = \sup_{1 \leq n \leq N} |P(\lambda_n)| \leq \sup_{0 \leq t \leq 2} |P(t)|. \quad (\text{III.5})$$

To estimate $\|\mathbf{A}\|_{\mathcal{B}_p}$, $p \neq 2$, of a graph filter $\mathbf{A} = (a(i, j))_{i, j \in V}$, we define the *bound* of \mathbf{A} by

$$\|\mathbf{A}\|_{\infty} = \sup_{i, j \in V} |a(i, j)|. \quad (\text{III.6})$$

A graph filter \mathbf{A} on ℓ^p , $1 \leq p \leq \infty$, has bounded entries and

$$\|\mathbf{A}\|_{\infty} \leq \sup_{j \in V} \|\mathbf{A}\mathbf{e}_j\|_p \leq \|\mathbf{A}\|_{\mathcal{B}_p}, \quad 1 \leq p \leq \infty, \quad (\text{III.7})$$

where the last inequality is obtained from (III.1) by replacing \mathbf{x} by the standard unit vector \mathbf{e}_j with j -th component taking value one while all others are zero.

For the distributed implementation for an NSGFB, bounded filters with finite bandwidth will be used as analysis filters, see Assumption IV.1.

Definition III.2. The *bandwidth* $\sigma := \sigma(\mathbf{A})$ of a graph filter $\mathbf{A} = (a(i, j))_{i, j \in V}$ is the minimal nonnegative integer such that $a(i, j) = 0$ for all $i, j \in V$ with $\rho(i, j) > \sigma$. For a filter pair (\mathbf{A}, \mathbf{B}) , we define its bandwidth $\sigma := \sigma(\mathbf{A}, \mathbf{B})$ by $\max(\sigma(\mathbf{A}), \sigma(\mathbf{B}))$.

In the following proposition, we show that a bounded filter with finite bandwidth is a graph filter on ℓ^p , $1 \leq p \leq \infty$, with filter bound dominated by some constant, independent of the size of the graph \mathcal{G} .

Proposition III.3. Let $1 \leq p \leq \infty$, and \mathcal{G} be a graph satisfying Assumptions II.1 and II.2. Then for any bounded graph filter \mathbf{A} with bandwidth σ , we have

$$\|\mathbf{A}\|_\infty \leq \|\mathbf{A}\|_{\mathcal{B}_p} \leq D_1(\mathcal{G})(\sigma + 1)^d \|\mathbf{A}\|_\infty, \quad (\text{III.8})$$

where d and $D_1(\mathcal{G})$ are the Beurling dimension and density of the graph \mathcal{G} respectively.

For $n \geq 1$, we define *spline filters* $\mathbf{H}_{0,n}^{\text{spln}}$ and $\mathbf{H}_{1,n}^{\text{spln}}$ of order n by

$$\mathbf{H}_{0,n}^{\text{spln}} = \left(\mathbf{I} - \frac{1}{2} \mathbf{L}_{\mathcal{G}}^{\text{sym}} \right)^n \quad \text{and} \quad \mathbf{H}_{1,n}^{\text{spln}} = \left(\frac{1}{2} \mathbf{L}_{\mathcal{G}}^{\text{sym}} \right)^n, \quad (\text{III.9})$$

see [39] in circulant graph setting. Spline filters $\mathbf{H}_{0,n}^{\text{spln}}$ and $\mathbf{H}_{1,n}^{\text{spln}}$, $n \geq 1$, have bandwidth n and their filter bounds on ℓ^2 dominated by one, i.e.,

$$\|\mathbf{H}_{l,n}^{\text{spln}}\|_{\mathcal{B}_2} \leq 1, \quad l = 0, 1. \quad (\text{III.10})$$

For $p \neq 2$, we obtain from Proposition III.3 that

$$\begin{aligned} \|\mathbf{H}_{l,n}^{\text{spln}}\|_{\mathcal{B}_p} &\leq \|\mathbf{H}_{l,1}^{\text{spln}}\|_{\mathcal{B}_p}^n \leq (2^d D_1(\mathcal{G}) \|\mathbf{H}_{l,1}^{\text{spln}}\|_\infty)^n \\ &= (2^{d-1} D_1(\mathcal{G}))^n, \quad l = 0, 1, \end{aligned} \quad (\text{III.11})$$

where d and $D_1(\mathcal{G})$ are the Beurling dimension and density of the graph \mathcal{G} respectively. Therefore our representative spline filters $\mathbf{H}_{0,n}^{\text{spln}}$ and $\mathbf{H}_{1,n}^{\text{spln}}$, $n \geq 1$, are graph filters on ℓ^p , $1 \leq p \leq \infty$, with filter bounds dominated by some constants independent of the size of the graph \mathcal{G} .

IV. ANALYSIS FILTER BANKS

The analysis filter bank decomposes the input signal on a graph into two components carrying frequency information. In this section, we design the analysis filter bank $(\mathbf{H}_0, \mathbf{H}_1)$ of an NSGFB to have small bandwidth, to pass/block the normalized constant signal, and to have stability on ℓ^2 , see Assumptions IV.1, IV.2 and IV.4. In this section, we also show that analysis filter banks have stability on ℓ^p for all $1 \leq p \leq \infty$, with an estimate on their lower and upper ℓ^p -stability bounds independent of the size of the graph, see Theorem IV.6.

Let $\mathcal{G} = (V, E)$ be a graph satisfying Assumptions II.1 and II.2, and $(\mathbf{H}_0, \mathbf{H}_1)$ be the analysis filter bank of an NSGFB. For the distributed implementation of an NSGFB, we make the following assumption for its analysis filter bank $(\mathbf{H}_0, \mathbf{H}_1)$.

Assumption IV.1. The analysis filter bank $(\mathbf{H}_0, \mathbf{H}_1)$ has bandwidth $\sigma \geq 1$.

Given an input graph signal $\mathbf{x} = (x_i)_{i \in V}$, outputs of analysis procedure are

$$\mathbf{z}_0 = \mathbf{H}_0 \mathbf{x} \quad \text{and} \quad \mathbf{z}_1 = \mathbf{H}_1 \mathbf{x}. \quad (\text{IV.1})$$

Write $\mathbf{z}_l = (z_l(i))_{i \in V}$ and $\mathbf{H}_l = (h_l(i, j))_{i, j \in V}$, $l = 0, 1$. Then it follows from (IV.1) and Assumption IV.1 that component values of the outputs \mathbf{z}_0 and \mathbf{z}_1 at each vertex $k \in V$ are weighted sums of values of the input \mathbf{x} in a σ -neighborhood of k ,

$$z_l(k) = \sum_{\rho(i,k) \leq \sigma} h_l(k, i) x(i), \quad i \in V. \quad (\text{IV.2})$$

Thus the analysis procedure of an NSGFB can be implemented in a distributed manner.

To apply an NSGFB to some real world applications, such as noise suppression and abnormal phenomenon detection, its analysis filter bank should constitute certain spectral decomposition ([20], [21], [23], [45]). Throughout the paper, we also make the following assumption for the analysis filter bank $(\mathbf{H}_0, \mathbf{H}_1)$.

Assumption IV.2. The filter \mathbf{H}_0 passes the normalized constant signal $\mathbf{D}_G^{1/2}\mathbf{1}$, and the filter \mathbf{H}_1 blocks the normalized constant signal $\mathbf{D}_G^{1/2}\mathbf{1}$, i.e.,

$$\mathbf{H}_0\mathbf{D}_G^{1/2}\mathbf{1} = \mathbf{D}_G^{1/2}\mathbf{1} \quad \text{and} \quad \mathbf{H}_1\mathbf{D}_G^{1/2}\mathbf{1} = \mathbf{0}. \quad (\text{IV.3})$$

The frequency partition of an analysis filter bank on an arbitrary graph \mathcal{G} is not as obvious as that in classical setting. For the case that

$$\mathbf{H}_0 = P_0(\mathbf{L}_G^{\text{sym}}) \quad \text{and} \quad \mathbf{H}_1 = P_1(\mathbf{L}_G^{\text{sym}}) \quad (\text{IV.4})$$

for some polynomials P_0 and P_1 , one may verify that Assumption IV.2 is satisfied if and only if

$$P_0(0) = 1 \quad \text{and} \quad P_1(0) = 0. \quad (\text{IV.5})$$

The above equivalence follows from the fact that $\mathbf{D}_G^{1/2}\mathbf{1}$ is an eigenvector of the symmetric normalized Laplacian $\mathbf{L}_G^{\text{sym}}$ associated with eigenvalue zero.

The spline filter banks $(\mathbf{H}_{0,n}^{\text{spln}}, \mathbf{H}_{1,n}^{\text{spln}})$, $n \geq 1$, are of the form (IV.4) with $P_0(t) = (1 - t/2)^n$ and $P_1(t) = (t/2)^n$, and they satisfy Assumption IV.2 by (IV.5), i.e.,

$$\mathbf{H}_{0,n}^{\text{spln}}\mathbf{D}_G^{1/2}\mathbf{1} = \mathbf{D}_G^{1/2}\mathbf{1} \quad \text{and} \quad \mathbf{H}_{1,n}^{\text{spln}}\mathbf{D}_G^{1/2}\mathbf{1} = \mathbf{0}. \quad (\text{IV.6})$$

Spline filter banks in the circulant graph setting are known in [39] as graph-spline wavelet transform. Shown in Figure 3 is local smoothing/blocking phenomenon of the spline filter bank $(\mathbf{H}_{0,2}^{\text{spln}}, \mathbf{H}_{1,2}^{\text{spln}})$ to a blockwise constant signal on the Minnesota traffic graph and a blockwise smooth signal on the random geometric graph RGG₄₀₉₆ in Figure 2. It is observed that the lowpass filtered signal is very close to the original signal except near the boundary between different blocks, and that the highpass filtered signal essentially vanishes except around the region where the original signal exhibits sharp local variation.

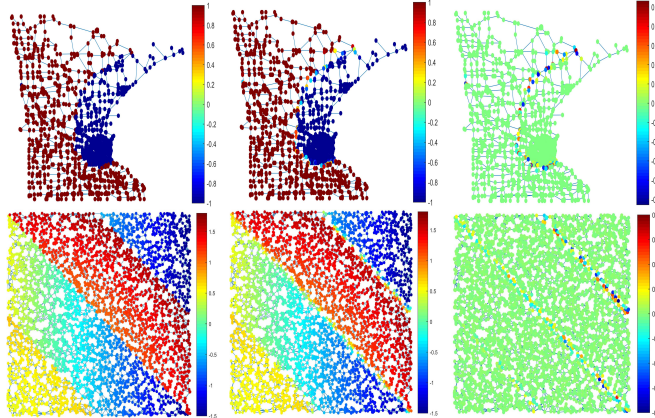


Fig. 3. Plotted on the top (resp. at the bottom), from left to right, are the original signal \mathbf{x} on the Minnesota traffic graph (resp. on the random geometric graph RGG₄₀₉₆ in Figure 2), the lowpass filtered signal $\mathbf{H}_{0,2}^{\text{spln}}\mathbf{x}$ and the highpass filtered signal $\mathbf{H}_{1,2}^{\text{spln}}\mathbf{x}$. The signal \mathbf{x} on the top is a blockwise constant function that has only two values ± 1 on three blocks with one block only containing a vertex ([20], [21]), and the signal \mathbf{x} at the bottom is a blockwise polynomial consisting of four strips and imposing the polynomial $0.5 - 2c_x$ on the first and third diagonal strips and $0.5 + c_x^2 + c_y^2$ on the second and fourth strips respectively, where (c_x, c_y) are the coordinates of vertices ([26]).

Robustness is a fundamental requirement in the context of filter bank to control the signal dynamic range and to regulate the input noise. For the robustness of an NSGFB on ℓ^p , $1 \leq p \leq \infty$, we introduce stability of a graph filter pair on ℓ^p .

Definition IV.3. Let $1 \leq p \leq \infty$. We say that $(\mathbf{H}_0, \mathbf{H}_1)$ is *stable on ℓ^p* if there are two positive constants C_p and D_p such that

$$C_p\|\mathbf{x}\|_p \leq (\|\mathbf{H}_0\mathbf{x}\|_p^p + \|\mathbf{H}_1\mathbf{x}\|_p^p)^{1/p} \leq D_p\|\mathbf{x}\|_p \quad (\text{IV.7})$$

hold for all $\mathbf{x} \in \ell^p$ if $1 \leq p < \infty$, and

$$C_\infty \|\mathbf{x}\|_\infty \leq \max(\|\mathbf{H}_0 \mathbf{x}\|_\infty, \|\mathbf{H}_1 \mathbf{x}\|_\infty) \leq D_\infty \|\mathbf{x}\|_\infty \quad (\text{IV.8})$$

hold for all $\mathbf{x} \in \ell^\infty$ if $p = \infty$. The optimal constants C_p and D_p for the inequalities in (IV.7) and (IV.8) to hold are called as *lower and upper stability bounds* of the graph filter bank $(\mathbf{H}_0, \mathbf{H}_1)$ on ℓ^p respectively.

Given an NSGFB with the analysis filter bank $(\mathbf{H}_0, \mathbf{H}_1)$ and synthesis filter bank $(\mathbf{G}_0, \mathbf{G}_1)$ such that the perfect reconstruction condition (I.1) holds, we have that

$$\begin{aligned} (\|\mathbf{G}_0\|_{\mathcal{B}_2}^2 + \|\mathbf{G}_1\|_{\mathcal{B}_2}^2)^{-1} \|\mathbf{x}\|_2^2 &\leq \|\mathbf{H}_0 \mathbf{x}\|_2^2 + \|\mathbf{H}_1 \mathbf{x}\|_2^2 \\ &\leq (\|\mathbf{H}_0\|_{\mathcal{B}_2}^2 + \|\mathbf{H}_1\|_{\mathcal{B}_2}^2) \|\mathbf{x}\|_2^2 \end{aligned}$$

hold for all $\mathbf{x} \in \ell^2$. So throughout the paper, we assume that the analysis procedure is stable on ℓ^2 .

Assumption IV.4. The analysis filter bank $(\mathbf{H}_0, \mathbf{H}_1)$ is stable on ℓ^2 .

For any $\mathbf{x} \in \ell^2$, direct calculation leads to

$$\|\mathbf{H}_0 \mathbf{x}\|_2^2 + \|\mathbf{H}_1 \mathbf{x}\|_2^2 = \mathbf{x}^T (\mathbf{H}_0^T \mathbf{H}_0 + \mathbf{H}_1^T \mathbf{H}_1) \mathbf{x}. \quad (\text{IV.9})$$

Thus we have the following characterization to Assumption IV.4.

Proposition IV.5. Let \mathcal{G} satisfy Assumptions II.1 and II.2. Then $(\mathbf{H}_0, \mathbf{H}_1)$ satisfies Assumption IV.4 if and only if $\mathbf{H} := \mathbf{H}_0^T \mathbf{H}_0 + \mathbf{H}_1^T \mathbf{H}_1$ is positive definite. Moreover, the optimal constants C_2 and D_2 for (IV.7) to hold can be evaluated by

$$C_2^2 = (\|\mathbf{H}^{-1}\|_{\mathcal{B}_2})^{-1} \quad \text{and} \quad D_2^2 = \|\mathbf{H}\|_{\mathcal{B}_2}. \quad (\text{IV.10})$$

For graph filters \mathbf{H}_0 and \mathbf{H}_1 of the form (IV.4), we obtain from (III.3) that

$$\mathbf{H}_0^T \mathbf{H}_0 + \mathbf{H}_1^T \mathbf{H}_1 = \mathbf{U}^T ((P_0(\boldsymbol{\Lambda}))^2 + (P_1(\boldsymbol{\Lambda}))^2) \mathbf{U}. \quad (\text{IV.11})$$

Hence we can evaluate the optimal constants C_2 and D_2 for (IV.7) to hold explicitly:

$$\begin{aligned} &\inf_{1 \leq m \leq N} (P_0(\lambda_m))^2 + (P_1(\lambda_m))^2 \\ &= \inf_{\|\mathbf{x}\|_2=1} \|\mathbf{H}_0 \mathbf{x}\|_2^2 + \|\mathbf{H}_1 \mathbf{x}\|_2^2 \leq \sup_{\|\mathbf{x}\|_2=1} \|\mathbf{H}_0 \mathbf{x}\|_2^2 + \|\mathbf{H}_1 \mathbf{x}\|_2^2 \\ &= \sup_{1 \leq m \leq N} (P_0(\lambda_m))^2 + (Q_0(\lambda_m))^2. \end{aligned} \quad (\text{IV.12})$$

Set $R_n(t) = (1 - t/2)^{2n} + (t/2)^{2n}$, $n \geq 1$. Then

$$\inf_{0 \leq t \leq 2} R_n(t) = 2^{-2n+1} \quad \text{and} \quad \sup_{0 \leq t \leq 2} R_n(t) = 1. \quad (\text{IV.13})$$

Taking $P_0(t) = (1 - t/2)^n$ and $P_1(t) = (t/2)^n$ in (IV.12) and applying (IV.13), we get

$$\begin{aligned} 2^{-2n+1} \|\mathbf{x}\|_2^2 &\leq \mathbf{x}^T ((\mathbf{H}_{0,n}^{\text{spln}})^T \mathbf{H}_{0,n}^{\text{spln}} + (\mathbf{H}_{1,n}^{\text{spln}})^T \mathbf{H}_{1,n}^{\text{spln}}) \mathbf{x} \\ &= \|\mathbf{H}_{0,n}^{\text{spln}} \mathbf{x}\|_2^2 + \|\mathbf{H}_{1,n}^{\text{spln}} \mathbf{x}\|_2^2 \leq \|\mathbf{x}\|_2^2 \end{aligned} \quad (\text{IV.14})$$

for all $\mathbf{x} \in \ell^2$. Therefore spline filter banks $(\mathbf{H}_{0,n}^{\text{spln}}, \mathbf{H}_{1,n}^{\text{spln}})$ of order $n \geq 1$ satisfy Assumption IV.4 with lower bound $2^{-n+1/2}$ and upper bound 1 by (IV.12) and (IV.14).

Filters in a stable filter bank on ℓ^p are graph filters on ℓ^p , $1 \leq p \leq \infty$. In the following theorem, we show that analysis filter banks are stable on ℓ^p , $1 \leq p \leq \infty$, with quantitative estimates on their lower and upper stability bounds by some constants independent of the size of the graph.

Theorem IV.6. Let \mathcal{G} be a graph satisfying Assumptions II.1 and II.2, \mathbf{H}_0 and \mathbf{H}_1 have bandwidth $\sigma \geq 1$, and set $\mathbf{H} := \mathbf{H}_0^T \mathbf{H}_0 + \mathbf{H}_1^T \mathbf{H}_1$. If $(\mathbf{H}_0, \mathbf{H}_1)$ is stable on ℓ^2 , then it is stable on ℓ^p for all $1 \leq p \leq \infty$. Moreover, we have the following estimates for its lower and upper stability bounds C_p and D_p :

$$C_p \geq \frac{\|\mathbf{H}\|_{\mathcal{B}_2}^{1/2}}{d!2^{d+1}(D_1(\mathcal{G}))^2(\sigma+1)^{2d}\kappa^{d+2}} \quad (\text{IV.15})$$

and

$$D_p \leq 2D_1(\mathcal{G})(\sigma+1)^d \|\mathbf{H}\|_{\mathcal{B}_2}^{1/2}, \quad (\text{IV.16})$$

where d and $D_1(\mathcal{G})$ are the Beurling dimension and density of the graph \mathcal{G} respectively, and

$$\kappa = \|\mathbf{H}^{-1}\|_{\mathcal{B}_2} \|\mathbf{H}\|_{\mathcal{B}_2} \quad (\text{IV.17})$$

is the condition number of the matrix \mathbf{H} .

Combining (IV.14) and Theorem IV.6, the spline filter banks $(\mathbf{H}_{0,n}^{\text{spln}}, \mathbf{H}_{1,n}^{\text{spln}})$, $n \geq 1$, are stable on ℓ^p , $1 \leq p \leq \infty$, and their lower and upper stability bounds C_p and D_p satisfy

$$\begin{aligned} \frac{1}{2^{2(d+2)n-1}d!(n+1)^{2d}(D_1(\mathcal{G}))^2} &\leq C_p \leq D_p \\ &\leq 2D_1(\mathcal{G})(n+1)^{d+1}. \end{aligned}$$

We finish this section with a remark on stability bounds of a graph filter bank on the space ℓ^2 and on the spaces ℓ^p , $p \neq 2$.

Remark IV.7. For a finite graph $\mathcal{G} = (V, E)$, a stable filter bank $(\mathbf{H}_0, \mathbf{H}_1)$ on ℓ^2 is also stable on ℓ^p , $1 \leq p \leq \infty$, and the lower stability bounds C_2 and C_p satisfy

$$N^{-|1/p-1/2|} \leq \frac{C_2}{C_p} \leq N^{|1/p-1/2|}, \quad (\text{IV.18})$$

where $N = \#V$ is the size of the graph \mathcal{G} . The above estimation is unfavorable when the graph \mathcal{G} has large size, however it cannot be improved if there is no restriction on the filter bank $(\mathbf{H}_0, \mathbf{H}_1)$. As our analysis filter bank $(\mathbf{H}_0, \mathbf{H}_1)$ has small bandwidth σ , we obtain the following estimate independent of the size N of the graph \mathcal{G} from Proposition IV.5 and Theorem IV.6,

$$\frac{1}{2D_1(\mathcal{G})(\sigma+1)^{d\kappa^{1/2}}} \leq \frac{C_2}{C_p} \leq d!2^{d+1}(D_1(\mathcal{G}))^2(\sigma+1)^{2d}\kappa^{d+3/2}, \quad (\text{IV.19})$$

where κ is given in (IV.17). The reader may refer to [5] and [40]–[44] for historical remarks and various estimates on the ratio between stability bounds on ℓ^p and ℓ^q , $1 \leq p, q \leq \infty$, for matrices with certain off-diagonal decay.

V. SYNTHESIS FILTER BANKS AND BEZOUT IDENTITY

Let $\mathcal{G} = (V, E)$ be a graph satisfying Assumptions II.1 and II.2, and $(\mathbf{H}_0, \mathbf{H}_1)$ be a graph filter bank satisfying Assumptions IV.1, IV.2 and IV.4. In this section, we propose an algebraic method to construct graph filters \mathbf{G}_0 and \mathbf{G}_1 so that the NSGFB with the analysis filter bank $(\mathbf{H}_0, \mathbf{H}_1)$ and synthesis filter bank $(\mathbf{G}_0, \mathbf{G}_1)$ satisfies the perfect reconstruction condition (I.1) and the bandwidth of synthesis filter bank $(\mathbf{G}_0, \mathbf{G}_1)$ is no larger than the bandwidth of the analysis filter bank $(\mathbf{H}_0, \mathbf{H}_1)$. The proposed approach applies for filter banks $(\mathbf{H}_0, \mathbf{H}_1)$ being polynomials of the symmetric normalized Laplacian on the graph \mathcal{G} , i.e.,

$$\mathbf{H}_0 = P_0(\mathbf{L}_{\mathcal{G}}^{\text{sym}}) \text{ and } \mathbf{H}_1 = P_1(\mathbf{L}_{\mathcal{G}}^{\text{sym}}) \quad (\text{V.1})$$

for some polynomials P_0 and P_1 .

Theorem V.1. Let \mathcal{G} be a graph satisfying Assumptions II.1 and II.2, $(\mathbf{H}_0, \mathbf{H}_1)$ be a graph filter bank satisfying Assumptions IV.1, IV.2 and IV.4 and being of the form (V.1), and let $0 \leq \lambda_1 \leq \lambda_2 \leq \dots \leq \lambda_N \leq 2$ be eigenvalues of the symmetric normalized Laplacian $\mathbf{L}_{\mathcal{G}}^{\text{sym}}$. If polynomials Q_0 and Q_1 satisfy

$$P_0(\lambda_m)Q_0(\lambda_m) + P_1(\lambda_m)Q_1(\lambda_m) = 1, \quad 1 \leq m \leq N, \quad (\text{V.2})$$

then the NSGFB with the analysis filter bank $(\mathbf{H}_0, \mathbf{H}_1)$ and synthesis filter bank $(\mathbf{G}_0, \mathbf{G}_1)$ satisfies the perfect reconstruction condition (I.1), where

$$\mathbf{G}_0 = Q_0(\mathbf{L}_{\mathcal{G}}^{\text{sym}}) \quad \text{and} \quad \mathbf{G}_1 = Q_1(\mathbf{L}_{\mathcal{G}}^{\text{sym}}). \quad (\text{V.3})$$

The filter \mathbf{G}_0 in (V.3) passes the normalized constant signal $\mathbf{D}_{\mathcal{G}}^{1/2}\mathbf{1}$, since $\mathbf{G}_0\mathbf{D}_{\mathcal{G}}^{1/2}\mathbf{1} = Q_0(0)\mathbf{D}_{\mathcal{G}}^{1/2}\mathbf{1} = \mathbf{D}_{\mathcal{G}}^{1/2}\mathbf{1}$, where the last equation follows from (IV.5) and (V.2). However, the filter \mathbf{G}_1 in (V.3) may not block the normalized constant signal, as $\mathbf{G}_1\mathbf{D}_{\mathcal{G}}^{1/2}\mathbf{1} = Q_1(0)\mathbf{D}_{\mathcal{G}}^{1/2}\mathbf{1}$ is not necessarily a zero signal. In this case, we can construct a new synthesis filter bank by lifting,

$$\tilde{\mathbf{G}}_0 = \mathbf{G}_0 + Q_1(0)\mathbf{H}_1 \quad \text{and} \quad \tilde{\mathbf{G}}_1 = \mathbf{G}_1 - Q_1(0)\mathbf{H}_0, \quad (\text{V.4})$$

which satisfies $\tilde{\mathbf{G}}_0\mathbf{D}_{\mathcal{G}}^{1/2}\mathbf{1} = \mathbf{D}_{\mathcal{G}}^{1/2}\mathbf{1}$ and $\tilde{\mathbf{G}}_1\mathbf{D}_{\mathcal{G}}^{1/2}\mathbf{1} = \mathbf{0}$.

A strong version of (V.2) is the Bezout identity

$$P_0(z)Q_0(z) + P_1(z)Q_1(z) = 1, \quad z \in \mathbb{C} \quad (\text{V.5})$$

for polynomials P_0, P_1, Q_0 and Q_1 . In the circulant graph setting, the above approach of constructing synthesis filter banks via solving Bezout identity (V.5) was discussed in [39]. Comparing with the Bezout identity (V.2) on the eigenvalue set of the symmetric normalized Laplacian matrix $\mathbf{L}_{\mathcal{G}}^{\text{sym}}$, the advantage of the approach (V.5) provides a tool to design synthesis filter banks without a priori knowledge of global topology of the residing graph and then it simplifies the design of synthesis filter banks for signal reconstruction. It is well known that the Bezout identity (V.5) is solvable if and only if polynomials P_0 and P_1 have no common root. Moreover, there is a unique solution pair $(Q_{0,B}, Q_{1,B})$ to the Bezout identity (V.5) such that $Q_{0,B}(0) = 1$, $Q_{1,B}(0) = 0$ and the degree of $Q_{0,B}$ (resp. $Q_{1,B}$) is no larger than the degree of P_1 (resp. P_0). Define

$$\mathbf{G}_{0,B} = Q_{0,B}(\mathbf{L}_{\mathcal{G}}^{\text{sym}}) \quad \text{and} \quad \mathbf{G}_{1,B} = Q_{1,B}(\mathbf{L}_{\mathcal{G}}^{\text{sym}}). \quad (\text{V.6})$$

Then the bandwidth of the synthesis filter bank $(\mathbf{G}_{0,B}, \mathbf{G}_{1,B})$ is no larger than bandwidth of the analysis filter bank $(\mathbf{H}_0, \mathbf{H}_1)$. Moreover, for any synthesis filter bank $(\mathbf{G}_0, \mathbf{G}_1)$ there exists a polynomial R such that

$$\mathbf{G}_0 = \mathbf{G}_{0,B} + R(\mathbf{L}_{\mathcal{G}}^{\text{sym}})\mathbf{H}_1 \quad \text{and} \quad \mathbf{G}_1 = \mathbf{G}_{1,B} - R(\mathbf{L}_{\mathcal{G}}^{\text{sym}})\mathbf{H}_0 \quad (\text{V.7})$$

satisfies the perfect reconstruction condition (I.1). We remark that the above polynomials R could be appropriately chosen for real world applications of an NSFGB.

Following (V.6), we define *synthesis spline filters* $\mathbf{G}_{0,n}^{\text{B,spln}}$ and $\mathbf{G}_{1,n}^{\text{B,spln}}$ of order $n \geq 1$ by

$$\mathbf{G}_{0,n}^{\text{B,spln}} = Q_{0,n}^{\text{B,spln}}(\mathbf{L}_{\mathcal{G}}^{\text{sym}}) \quad \text{and} \quad \mathbf{G}_{1,n}^{\text{B,spln}} = Q_{1,n}^{\text{B,spln}}(\mathbf{L}_{\mathcal{G}}^{\text{sym}}), \quad (\text{V.8})$$

where

$$Q_{0,n}^{\text{B,spln}}(t) = \sum_{l=0}^{n-1} \binom{2n-1}{l} \left(1 - \frac{t}{2}\right)^{n-1-l} \left(\frac{t}{2}\right)^l + \binom{2n-1}{n-1} \left(\frac{t}{2}\right)^n$$

and

$$Q_{1,n}^{\text{B,spln}}(t) = \sum_{l=0}^{n-1} \binom{2n-1}{l} \left(\frac{t}{2}\right)^{n-1-l} \left(1 - \frac{t}{2}\right)^l - \binom{2n-1}{n-1} \left(1 - \frac{t}{2}\right)^n.$$

For $n \geq 1$, the filter $\mathbf{G}_{0,n}^{\text{B,spln}}$ passes the normalized constant signal $\mathbf{D}_{\mathcal{G}}^{1/2} \mathbf{1}$, the filter $\mathbf{G}_{1,n}^{\text{B,spln}}$ blocks the normalized constant signal $\mathbf{D}_{\mathcal{G}}^{1/2} \mathbf{1}$, and the NSGFB with the analysis spline bank $(\mathbf{H}_{0,n}^{\text{spln}}, \mathbf{H}_{1,n}^{\text{spln}})$ and synthesis filter bank $(\mathbf{G}_{0,n}^{\text{B,spln}}, \mathbf{G}_{1,n}^{\text{B,spln}})$ satisfies the perfect reconstruction condition (I.1). The first two results follow from $Q_{0,n}^{\text{B,spln}}(0) = 1$ and $Q_{1,n}^{\text{B,spln}}(0) = 0$, while the perfect reconstruction conclusion holds since

$$\begin{aligned} & \left(1 - \frac{t}{2}\right)^n Q_{0,n}^{\text{B,spln}}(t) + \left(\frac{t}{2}\right)^n Q_{1,n}^{\text{B,spln}}(t) \\ &= \sum_{l=0}^{n-1} \binom{2n-1}{l} (1-u)^{2n-1-l} u^l \\ & \quad + \sum_{l=0}^{n-1} \binom{2n-1}{l} (1-u)^l u^{2n-1-l} \\ &= ((1-u) + u)^{2n-1} = 1, \end{aligned}$$

where $u = t/2$.

In real world applications of an NSGFB such as the proposed distributed denoising in Section VIII, the subband signals \mathbf{z}_0 and \mathbf{z}_1 in (IV.1) are processed via some (non)linear procedure, such as hard/soft thresholding and quantization. In this case, the reconstructed signal $\tilde{\mathbf{x}}$ is not necessarily the same as the original signal \mathbf{x} . In the following theorem, we show that the difference is mainly dominated by the error caused by the subband processing.

Proposition V.2. Let the graph \mathcal{G} , the analysis filter bank $(\mathbf{H}_0, \mathbf{H}_1)$ and the synthesis filter bank $(\mathbf{G}_0, \mathbf{G}_1)$ be as in Theorem V.1. Assume that the error caused by the subband processing Ψ_l on subband signals $\mathbf{z}_l = \mathbf{H}_l \mathbf{x}$, $l = 0, 1$, is dominated by ϵ for any input signal $\mathbf{x} \in \ell^p$, i.e.,

$$\|\mathbf{z}_l - \Psi_l(\mathbf{z}_l)\|_p \leq \epsilon, \quad l = 0, 1, \quad (\text{V.9})$$

where $\epsilon \geq 0$ and $1 \leq p \leq \infty$. For the input signal $\mathbf{x} \in \ell^p$, the reconstructed signal $\tilde{\mathbf{x}} = \mathbf{G}_0 \Psi_0(\mathbf{z}_0) + \mathbf{G}_1 \Psi_1(\mathbf{z}_1)$ via the corresponding NSGFB belongs to ℓ^p as well. Moreover

$$\|\tilde{\mathbf{x}} - \mathbf{x}\|_p \leq D_1(\mathcal{G})(\tilde{\sigma} + 1)^d (\|\mathbf{G}_0\|_\infty + \|\mathbf{G}_1\|_\infty) \epsilon, \quad (\text{V.10})$$

where d and $D_1(\mathcal{G})$ are the Beurling dimension and density of the graph \mathcal{G} respectively, and $\tilde{\sigma}$ is the bandwidth of the synthesis filter bank $(\mathbf{G}_0, \mathbf{G}_1)$.

We finish this section with a distributed implementation of the NSGFB with analysis/synthesis filter banks selected in Theorem V.1. Write $\mathbf{G}_l = (g_l(i, j))_{i,j \in V}$, $l = 0, 1$. As the synthesis filters \mathbf{G}_0 and \mathbf{G}_1 have finite bandwidth $\tilde{\sigma}$, the synthesis procedure can be implemented in a distributed manner,

$$\tilde{x}_k = \sum_{\rho(j,k) \leq \tilde{\sigma}} (g_0(k, j) \tilde{z}_0(j) + g_1(k, j) \tilde{z}_1(j)), \quad k \in V, \quad (\text{V.11})$$

where $\tilde{\mathbf{x}} = (\tilde{x}_i)_{i \in V}$ is the reconstructed signal and $\Psi_l(\mathbf{z}_l) = (\tilde{z}_l(i))_{i \in V}$, $l = 0, 1$, are outputs of subband processing. Hence values of the reconstructed signals $\tilde{\mathbf{x}}$ at each vertex $k \in V$ are weighted sums of values of the subband processed outputs $\Psi_0(\mathbf{z}_0)$ and $\Psi_1(\mathbf{z}_1)$ in a $\tilde{\sigma}$ -neighborhood of $k \in V$, cf. (IV.2) for distributed implementation of the analysis procedure.

Our representative subband processing procedures Ψ are hard(soft) thresholding and uniform quantization. For those cases, the subband processing Ψ is of the form $\Psi(\mathbf{z}) = (\psi(z_i))_{i \in V}$ for $\mathbf{z} = (z_i)_{i \in V}$, where ψ is the hard(soft) thresholding and uniform quantization function. Thus the subband processing can be implemented in a distributed manner and the error resulted are bounded (i.e., (V.9) holds for $p = \infty$) by the hard(soft) thresholding and quantization level. This together with (IV.2) and (V.11) implies that the NSGFB with analysis/synthesis filter banks in Theorem V.1 can be implemented in a distributed manner too, provided that the subband processing can be.

VI. SYNTHESIS FILTER BANK AND OPTIMIZATION

Let $\mathcal{G} = (V, E)$ be a graph satisfying Assumptions II.1 and II.2, and $(\mathbf{H}_0, \mathbf{H}_1)$ be a graph filter bank satisfying Assumptions IV.1, IV.2 and IV.4. In this section, we consider the construction of synthesis filter banks $(\mathbf{G}_0, \mathbf{G}_1)$ of an NSGFB by solving the minimization problem:

$$\underset{\mathbf{G}_0, \mathbf{G}_1}{\text{minimize}} \quad \|\mathbf{G}_0\|_F^2 + \|\mathbf{G}_1\|_F^2 \quad (\text{VI.1})$$

subject to the perfect reconstruction condition

$$\mathbf{G}_0 \mathbf{H}_0 + \mathbf{G}_1 \mathbf{H}_1 = \mathbf{I}. \quad (\text{VI.2})$$

Define the Lagrange function \mathcal{L} of the constrained optimization problem (VI.1) and (VI.2) by

$$\begin{aligned} \mathcal{L}(\mathbf{G}_0, \mathbf{G}_1, \boldsymbol{\Theta}) &= \|\mathbf{G}_0\|_F^2 + \|\mathbf{G}_1\|_F^2 \\ &\quad - \text{tr}((\mathbf{G}_0 \mathbf{H}_0 + \mathbf{G}_1 \mathbf{H}_1 - \mathbf{I}) \boldsymbol{\Theta}^T). \end{aligned}$$

By direct calculation, we have

$$\begin{cases} \frac{\partial \mathcal{L}}{\partial \mathbf{G}_0} = 2\mathbf{G}_0 - \boldsymbol{\Theta} \mathbf{H}_0^T \\ \frac{\partial \mathcal{L}}{\partial \mathbf{G}_1} = 2\mathbf{G}_1 - \boldsymbol{\Theta} \mathbf{H}_1^T \\ \frac{\partial \mathcal{L}}{\partial \boldsymbol{\Theta}} = \mathbf{G}_0 \mathbf{H}_0 + \mathbf{G}_1 \mathbf{H}_1 - \mathbf{I}. \end{cases} \quad (\text{VI.3})$$

Set $\mathbf{H} = \mathbf{H}_0^T \mathbf{H}_0 + \mathbf{H}_1^T \mathbf{H}_1$. Solving

$$\frac{\partial \mathcal{L}}{\partial \mathbf{G}_0} = \frac{\partial \mathcal{L}}{\partial \mathbf{G}_1} = \frac{\partial \mathcal{L}}{\partial \boldsymbol{\Theta}} = \mathbf{0}$$

leads to the unique solution of the constrained optimization problem (VI.1) and (VI.2),

$$\mathbf{G}_{0,L} = \mathbf{H}^{-1} \mathbf{H}_0^T \quad \text{and} \quad \mathbf{G}_{1,L} = \mathbf{H}^{-1} \mathbf{H}_1^T. \quad (\text{VI.4})$$

The synthesis filter bank $(\mathbf{G}_{0,L}, \mathbf{G}_{1,L})$ in (VI.4) satisfies

$$\mathbf{G}_{0,L} \mathbf{H}_0 + \mathbf{G}_{1,L} \mathbf{H}_1 = \mathbf{I},$$

and the filter $\mathbf{G}_{0,L}$ passes the normalized constant signal $\mathbf{D}_{\mathcal{G}}^{1/2} \mathbf{1}$, since

$$\mathbf{G}_{0,L} \mathbf{D}_{\mathcal{G}}^{1/2} \mathbf{1} = \mathbf{H}^{-1} (\mathbf{H}_0^T \mathbf{H}_0 + \mathbf{H}_1^T \mathbf{H}_1) \mathbf{D}_{\mathcal{G}}^{1/2} \mathbf{1} = \mathbf{D}_{\mathcal{G}}^{1/2} \mathbf{1}.$$

We remark that $\mathbf{G}_{1,L}$ may not block the normalized constant signal $\mathbf{D}_{\mathcal{G}}^{1/2} \mathbf{1}$.

For the case that \mathbf{H} is a diagonal matrix, the synthesis filter bank $(\mathbf{G}_{0,L}, \mathbf{G}_{1,L})$ in (VI.4) has the same bandwidth as the analysis filter bank $(\mathbf{H}_0, \mathbf{H}_1)$, and

$$|g_{l,L}(i, j)| \leq \begin{cases} \|\mathbf{H}^{-1}\|_{\mathcal{B}_2} \|\mathbf{H}_l\|_{\infty} & \text{if } \rho(i, j) \leq \sigma \\ 0 & \text{otherwise,} \end{cases} \quad (\text{VI.5})$$

where $\mathbf{G}_{l,L} := (g_{l,L}(i, j))_{i, j \in V}$, $l = 0, 1$.

Let κ be the condition number of the matrix \mathbf{H} in (IV.17). It is well known that $\kappa > 1$ when \mathbf{H} is not a diagonal matrix. For $\kappa > 1$, the synthesis filter bank $(\mathbf{G}_{0,L}, \mathbf{G}_{1,L})$ in (VI.4) does not necessarily have a small bandwidth, however it always has an exponential off-diagonal decay.

Theorem VI.1. Let $\mathcal{G} = (V, E)$ be a graph satisfying Assumptions II.1 and II.2, $(\mathbf{H}_0, \mathbf{H}_1)$ be a graph filter bank satisfying Assumptions IV.1, IV.2 and IV.4, κ be the condition number of the matrix $\mathbf{H} := \mathbf{H}_0^T \mathbf{H}_0 + \mathbf{H}_1^T \mathbf{H}_1$, and let $\mathbf{G}_{l,L} := (g_{l,L}(i, j))_{i,j \in V}, l = 0, 1$, be as in (VI.4). Assume that $\kappa > 1$, then

$$|g_{l,L}(i, j)| \leq D_1(\mathcal{G})(\sigma + 1)^d (1 - 1/\kappa)^{-1/2} \times \|\mathbf{H}^{-1}\|_{\mathcal{B}_2} \|\mathbf{H}_l\|_{\infty} \exp\left(-\frac{\theta}{2\sigma} \rho(i, j)\right) \quad (\text{VI.6})$$

hold for all $i, j \in V$ and $l = 0, 1$, where $\theta = \ln(\kappa/(\kappa - 1))$, $\sigma \geq 1$ is the bandwidth of the analysis filter bank $(\mathbf{H}_0, \mathbf{H}_1)$, and d and $D_1(\mathcal{G})$ are the Beurling dimension and density of the graph \mathcal{G} respectively.

Remark VI.2. Agents located at some vertices may lose data processing ability and/or communication capability. In that case, outputs of the analysis procedure of an NSGFB can be considered as being corrupted by shot noise. The exponential off-diagonal decay property in Theorem VI.1 implies that the reconstructed signal suffers mainly in their neighborhood of limited size. This means that the proposed NSGFB can limit the influence of shot noise essentially to their small neighborhoods on the graph.

Remark VI.3. By the exponential off-diagonal decay property in Theorem VI.1, the synthesis filters $(\mathbf{G}_{0,L}, \mathbf{G}_{1,L})$ are filters on $\ell^p, 1 \leq p \leq \infty$,

$$\|\mathbf{G}_{l,L}\|_{\mathcal{B}_p} \leq d! 2^d (D_1(\mathcal{G}))^2 (\sigma + 1)^{2d} \kappa^{d+1} (1 - 1/\kappa)^{-1/2} \times \|\mathbf{H}^{-1}\|_{\mathcal{B}_2} \|\mathbf{H}_l\|_{\infty}, \quad l = 0, 1. \quad (\text{VI.7})$$

The above conclusion with $p = \infty$ indicates that the NSGFB does not have a resonance effect.

Applying similar argument used in the proof of Proposition V.2, we have

Corollary VI.4. Let $\mathcal{G}, (\mathbf{H}_0, \mathbf{H}_1), (\mathbf{G}_{0,L}, \mathbf{G}_{1,L})$ be as in Theorem VI.1, and let $p, \Psi_0, \Psi_1, \epsilon$ be as in Proposition V.2. Assume that the input signal \mathbf{x} of the corresponding NSGFB belongs to ℓ^p , then the reconstructed signal $\tilde{\mathbf{x}} = \mathbf{G}_{0,L} \Psi_0(\mathbf{H}_0 \mathbf{x}) + \mathbf{G}_{1,L} \Psi_1(\mathbf{H}_1 \mathbf{x})$ via the NSGFB belongs to ℓ^p and

$$\|\tilde{\mathbf{x}} - \mathbf{x}\|_p \leq d! 2^d (D_1(\mathcal{G}))^2 (\sigma + 1)^{2d} \kappa^{d+1} \|\mathbf{H}^{-1}\|_{\mathcal{B}_2} \times (1 - 1/\kappa)^{-1/2} (\|\mathbf{H}_0\|_{\infty} + \|\mathbf{H}_1\|_{\infty}) \epsilon. \quad (\text{VI.8})$$

Solving the constrained optimization program (VI.1) and (VI.2) associated with the analysis spline filter banks $(\mathbf{H}_{0,n}^{\text{spln}}, \mathbf{H}_{1,n}^{\text{spln}})$, we obtain the synthesis spline filter bank $(\mathbf{G}_{0,n}^{\text{L,spln}}, \mathbf{G}_{1,n}^{\text{L,spln}}), n \geq 1$, where

$$\mathbf{G}_{l,n}^{\text{L,spln}} = \left((\mathbf{H}_{0,n}^{\text{spln}})^2 + (\mathbf{H}_{1,n}^{\text{spln}})^2 \right)^{-1} \mathbf{H}_{l,n}^{\text{spln}}, \quad l = 0, 1. \quad (\text{VI.9})$$

The synthesis spline filters $\mathbf{G}_{0,n}^{\text{L,spln}}$ and $\mathbf{G}_{1,n}^{\text{L,spln}}, n \geq 1$, have full bandwidth, however they have exponential off-diagonal decay. Write $\mathbf{G}_{l,n}^{\text{L,spln}} = (g_{l,n}^{\text{L,spln}}(i, j))_{i,j \in V}, l = 0, 1$. By (VI.6) and Theorem VI.1, we obtain that

$$|g_{l,n}^{\text{L,spln}}(i, j)| \leq 2^{3n-3/2} (2^{2n-1} - 1)^{-1/2} (n+1)^d D_1(\mathcal{G}) \times \exp\left(-\frac{\ln(2^{2n-1}/(2^{2n-1} - 1))}{2n} \rho(i, j)\right)$$

hold for all $i, j \in V$ and $l = 0, 1$.

By (III.4), we may use $P(\boldsymbol{\lambda})$ to describe frequency response of a filter $\mathbf{A} = P(\mathbf{L}_{\mathcal{G}}^{\text{sym}})$ of the form (III.2), where the vector $\boldsymbol{\lambda} = (\lambda_1, \dots, \lambda_N)$ is composed of eigenvalues $0 \leq \lambda_1 \leq \lambda_2 \leq \dots \leq \lambda_N \leq 2$ of the symmetric normalized Laplacian $\mathbf{L}_{\mathcal{G}}^{\text{sym}}$. Shown in Figure 4 are frequency responses of the analysis spline filter banks $(\mathbf{H}_{0,n}^{\text{spln}}, \mathbf{H}_{1,n}^{\text{spln}})$ of order n , the synthesis spline filter banks $(\mathbf{G}_{0,n}^{\text{B,spln}}, \mathbf{G}_{1,n}^{\text{B,spln}})$ in (V.8), and the synthesis spline filter banks $(\mathbf{G}_{0,n}^{\text{L,spln}}, \mathbf{G}_{1,n}^{\text{L,spln}})$ just constructed, where $n = 1, 2$. It is observed that the frequency responses of analysis spline filter banks $(\mathbf{H}_{0,n}^{\text{spln}}, \mathbf{H}_{1,n}^{\text{spln}})$ and synthesis spline filter banks $(\mathbf{G}_{0,n}^{\text{L,spln}}, \mathbf{G}_{1,n}^{\text{L,spln}})$ have certain complementary property, while the synthesis spline filter banks $(\mathbf{G}_{0,n}^{\text{B,spln}}, \mathbf{G}_{1,n}^{\text{B,spln}})$ constructed via solving a Bezout identity do not.

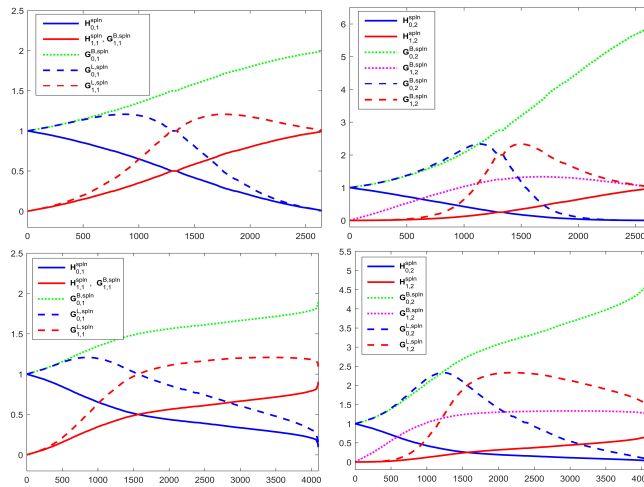


Fig. 4. Plotted on the top (resp. at the bottom) are the frequency responses of analysis/synthesis spline filters of order n on the Minnesota traffic graph (resp. on the random geometric graph RGG₄₀₉₆ in Figure 2), where $n = 1$ for the left figure and $n = 2$ for the right figure.

VII. ITERATIVE DISTRIBUTED ALGORITHM FOR SYNTHESIS PROCEDURE

For the NSGFB with synthesis filter banks in Theorem V.1, the distributed implementation of the corresponding synthesis procedure has been discussed in (V.11).

For the NSGFB with the analysis filter bank $(\mathbf{H}_0, \mathbf{H}_1)$ and synthesis filter bank $(\mathbf{G}_{0,L}, \mathbf{G}_{1,L})$ obtained from solving the constrained optimization problem (VI.1) and (VI.2), output $\tilde{\mathbf{x}}$ of the synthesis procedure is

$$\tilde{\mathbf{x}} = \mathbf{G}_{0,L}\tilde{\mathbf{z}}_0 + \mathbf{G}_{1,L}\tilde{\mathbf{z}}_1, \quad (\text{VII.1})$$

where $\tilde{\mathbf{z}}_0$ and $\tilde{\mathbf{z}}_1$ be outputs of subband processing. As filters $\mathbf{G}_{0,L}$ and $\mathbf{G}_{1,L}$ may have full bandwidth, it is infeasible to evaluate $\mathbf{G}_{0,L}\tilde{\mathbf{z}}_0$ and $\mathbf{G}_{1,L}\tilde{\mathbf{z}}_1$ directly in a distributed manner. In this paper, we do not intend to find synthesis filters $\mathbf{G}_{0,L}$ and $\mathbf{G}_{1,L}$ explicitly, instead we propose an iterative distributed algorithm to implement the synthesis procedure (VII.1).

The proposed iterative distributed algorithm is based on two pivoting observations. The first observation is that the output signal $\tilde{\mathbf{x}}$ in (VII.1) is the unique solution of the following global least squares problem:

$$\min_{\mathbf{x}} \|\mathbf{H}_0\mathbf{x} - \tilde{\mathbf{z}}_0\|_2^2 + \|\mathbf{H}_1\mathbf{x} - \tilde{\mathbf{z}}_1\|_2^2, \quad (\text{VII.2})$$

which follows from (VI.4). To solve the global optimization problem (VII.2) in a distributed manner, we introduce a family of local least squares problems,

$$\min_{\mathbf{x}} \|\mathbf{H}_0\chi_k^{2r}\mathbf{x} - \tilde{\mathbf{z}}_0\|_2^2 + \|\mathbf{H}_1\chi_k^{2r}\mathbf{x} - \tilde{\mathbf{z}}_1\|_2^2, \quad k \in V, \quad (\text{VII.3})$$

where $\chi_k^r, k \in V$, are truncation operators defined by

$$\chi_k^r : (x(i))_{i \in V} \mapsto (x(i)\chi_{B(k,r)}(i))_{i \in V}, \quad (\text{VII.4})$$

and $r \geq 1$ is a radius parameter to be determined later [5]. One may verify that given any $k \in V$, the unique solution of the local optimization problem (VII.3) is given by

$$\mathbf{v}_{k,r} = \chi_k^{2r} (\chi_k^{2r} \mathbf{H} \chi_k^{2r})^{-1} \chi_k^{2r} (\mathbf{H}_0^T \tilde{\mathbf{z}}_0 + \mathbf{H}_1^T \tilde{\mathbf{z}}_1), \quad (\text{VII.5})$$

where $\mathbf{H} = \mathbf{H}_0^T \mathbf{H}_0 + \mathbf{H}_1^T \mathbf{H}_1$. The second crucial observation is that the unique solution $\mathbf{v}_{k,r}$ of the local least squares problem (VII.3) in the $(2r)$ -neighborhood of the vertex k provides a local approximation

to the solution $\tilde{\mathbf{x}}$ of the global least squares problem (VII.2) in a r -neighborhood of the vertex $k \in V$. Therefore we can patch $\mathbf{v}_{k,r}, k \in V$, together

$$\mathbf{v}_r = \left(\sum_{k' \in V} \chi_{k'}^r \right)^{-1} \sum_{k \in V} \chi_k^r \mathbf{v}_{k,r} \quad (\text{VII.6})$$

to generate an approximation to the solution $\tilde{\mathbf{x}}$ of the global least squares problem (VII.2) in ℓ^p norm, i.e., there exists $\delta_{r,\sigma} \in (0, 1)$ such that

$$\|\mathbf{v}_r - \tilde{\mathbf{x}}\|_p \leq \delta_{r,\sigma} \|\tilde{\mathbf{x}}\|_p \quad (\text{VII.7})$$

when the radius parameter $r \geq 1$ is chosen appropriately. Set

$$\mathbf{J} = \left(\sum_{k' \in V} \chi_{k'}^r \right)^{-1} \sum_{k \in V} \chi_k^r (\chi_k^{2r} \mathbf{H} \chi_k^{2r})^{-1} \chi_k^{2r}. \quad (\text{VII.8})$$

Based on (VII.5), (VII.6) and (VII.7), we propose the following iterative distributed algorithm with initials $\tilde{\mathbf{z}}_0, \tilde{\mathbf{z}}_1 \in \ell^p$:

$$\begin{cases} \mathbf{v}^{(m)} = \mathbf{J}(\mathbf{H}_0^T \tilde{\mathbf{z}}_0^{(m-1)} + \mathbf{H}_1^T \tilde{\mathbf{z}}_1^{(m-1)}) \\ \tilde{\mathbf{z}}_0^{(m)} = \tilde{\mathbf{z}}_0^{(m-1)} - \mathbf{H}_0 \mathbf{v}^{(m)} \\ \tilde{\mathbf{z}}_1^{(m)} = \tilde{\mathbf{z}}_1^{(m-1)} - \mathbf{H}_1 \mathbf{v}^{(m)} \\ \mathbf{x}^{(m)} = \mathbf{x}^{(m-1)} + \mathbf{v}^{(m)} \end{cases} \quad (\text{VII.9})$$

for $m \geq 1$, where

$$\mathbf{x}^{(0)} = \mathbf{0}, \tilde{\mathbf{z}}_0^{(0)} = \tilde{\mathbf{z}}_0, \tilde{\mathbf{z}}_1^{(0)} = \tilde{\mathbf{z}}_1. \quad (\text{VII.10})$$

Remark VII.1. Decompose $\mathbf{H} = \mathbf{D} + \mathbf{R}$ into a diagonal component \mathbf{D} and the remainder \mathbf{R} . Then the classical Jacobi method to solve the linear system $\mathbf{H}\mathbf{x} = \mathbf{H}_0^T \tilde{\mathbf{z}}_0 + \mathbf{H}_1^T \tilde{\mathbf{z}}_1$ is

$$\mathbf{x}^{(m)} = \mathbf{D}^{-1}(\mathbf{H}_0^T \tilde{\mathbf{z}}_0 + \mathbf{H}_1^T \tilde{\mathbf{z}}_1 - \mathbf{R}\mathbf{x}^{(m-1)}), \quad m \geq 1. \quad (\text{VII.11})$$

The above iterative method converges when \mathbf{H} is diagonally dominated, which is not necessarily true for the case in our setting. We observe that for $r = 0$, the matrix \mathbf{J} in (VII.8) is equal to \mathbf{D}^{-1} . Hence the sequence $\mathbf{x}^{(m)}, m \geq 0$, in the proposed algorithm (VII.9) and (VII.10) with $r = 0$ is the same as the one in the Jacobi method (VII.11) with initial $\mathbf{x}^{(0)} = \mathbf{0}$.

Write $\mathbf{H}_l = (h_l(i, j))_{i, j \in V}$ and $\tilde{\mathbf{z}}_l = (\tilde{z}_l(i))_{i \in V}$, $l = 0, 1$. For the distributed implementation of the iterative algorithm (VII.9) and (VII.10), each agent $k \in V$ is required to transmit information to its neighboring vertices in $B(k, 2r + 2\sigma)$, and to store the number $m_k = \mu(B(k, r))$ of its neighboring vertices in $B(k, r)$ and four matrices $\mathbf{H}_{l,k} = (h_l(i, j))_{i \in B(k, 2r+\sigma), j \in B(k, 2r)}$ and $\tilde{\mathbf{H}}_{l,k} = (h_l(i, j))_{i \in B(k, 2r+\sigma), j \in B(k, 2r+2\sigma)}$, $l = 0, 1$. Shown in Algorithm VII.1 is a distributed implementation of the iterative algorithm (VII.9) and (VII.10), where every vertex $k \in V$ is required to store data of size $O((r + \sigma)^{2d})$, to perform $O((r + \sigma)^{2d})$ algebraic manipulations in each iteration, and to transmit data to its $(2r + 2\sigma)$ -neighborhood twice in each iteration.

In the next theorem, we further show that the iterative algorithm (VII.9) and (VII.10) converges exponentially when r is appropriately selected.

Theorem VII.2. Let $1 \leq p \leq \infty$, \mathcal{G} be a graph satisfying Assumptions II.1 and II.2, $(\mathbf{H}_0, \mathbf{H}_1)$ be a graph filter bank satisfying Assumptions IV.1, IV.2 and IV.4, $\kappa > 1$ be as (IV.17), the condition number of the matrix $\mathbf{H} := \mathbf{H}_0^T \mathbf{H}_0 + \mathbf{H}_1^T \mathbf{H}_1$, and let $(\mathbf{G}_{0,L}, \mathbf{G}_{1,L})$ be as in (VI.4). Set

$$\delta_{r,\sigma} := \frac{(D_1(\mathcal{G}))^2 (2\sigma + 1)^d \kappa^2}{\kappa - 1} \exp\left(-\frac{\theta}{2\sigma} r\right) (3r + 2\sigma + 1)^d, \quad (\text{VII.12})$$

Algorithm VII.1 Iterative Distributed Reconstruction Algorithm

Inputs: stop criterion ε and observations $\tilde{\mathbf{z}}_{l,k} = (\tilde{z}_l(i))_{i \in B(k, 2r+\sigma)}$ for $l = 0, 1$.

Operation: Compute $\mathbf{F}_k = \mathbf{H}_{0,k}^T \mathbf{H}_{0,k} + \mathbf{H}_{1,k}^T \mathbf{H}_{1,k}$, find its inverse $(\mathbf{F}_k)^{-1}$, and then compute $\mathbf{G}_{l,L;k} := (\mathbf{F}_k)^{-1} \mathbf{H}_{l,k}^T$, $l = 0, 1$.

Initialization: $\mathbf{x}_k^{(0)} = \mathbf{0}$, $\tilde{\mathbf{z}}_{0,k}^{(0)} = \tilde{\mathbf{z}}_{0,k}$ and $\tilde{\mathbf{z}}_{1,k}^{(0)} = \tilde{\mathbf{z}}_{1,k}$.

Iteration:

1) $\mathbf{u}_k = \mathbf{G}_{0,L;k} \tilde{\mathbf{z}}_{0,k}^{(m)} + \mathbf{G}_{1,L;k} \tilde{\mathbf{z}}_{1,k}^{(m)}$ and write $\mathbf{u}_k = (u_k(i))_{i \in B(k, 2r)}$.

2) Communicate to all vertices $i \in B(k, r) \setminus \{k\}$ to send data $u_k(i)$ and receive data $u_i(k)$.

3) Produce $v(k) = \frac{1}{m_k} \sum_{i \in B(k, r)} u_i(k)$.

4) Communicate to all vertices $i \in B(k, 2r + 2\sigma) \setminus \{k\}$ to send data $v(k)$ and receive data $v(i)$, and then generate a vector $\mathbf{v}_k = (v(i))_{i \in B(k, 2r+2\sigma)}$.

5) Update $\mathbf{x}_k^{(m+1)} = \mathbf{x}_k^{(m)} + \mathbf{v}_k$ and $\tilde{\mathbf{z}}_{l,k}^{(m+1)} = \tilde{\mathbf{z}}_{l,k}^{(m)} - \tilde{\mathbf{H}}_{l,k} \mathbf{v}_k$, $l = 0, 1$.

6) Evaluate $\|\mathbf{v}_k\|_\infty \leq \varepsilon$. If yes, terminate the iteration and output $\mathbf{x}_k^{(m+1)}$. Otherwise, set $m = m + 1$.

Outputs: $\mathbf{x}_k^{(m+1)}$.

where $\theta = \ln(\kappa/(\kappa - 1))$, $\sigma \geq 1$ is the bandwidth of the analysis filter bank $(\mathbf{H}_0, \mathbf{H}_1)$, and d and $D_1(\mathcal{G})$ are the Beurling dimension and density of the graph \mathcal{G} respectively. Take $\tilde{\mathbf{z}}_0, \tilde{\mathbf{z}}_1 \in \ell^p$, and let $\mathbf{x}^{(m)}$, $m \geq 0$, be as in (VII.9) and (VII.10). If the radius parameter r is so chosen that

$$\delta_{r,\sigma} \in (0, 1), \quad (\text{VII.13})$$

then $\mathbf{x}^{(m)}$, $m \geq 0$, converges to the least squares solution $\tilde{\mathbf{x}}$ in (VII.1) exponentially,

$$\|\mathbf{x}^{(m)} - \tilde{\mathbf{x}}\|_p \leq (\delta_{r,\sigma})^m \|\tilde{\mathbf{x}}\|_p, \quad m \geq 0. \quad (\text{VII.14})$$

Remark VII.3. For $l = 0, 1$, we can apply (VII.9) to prove by induction on m that

$$\tilde{\mathbf{z}}_l^{(m)} - (\tilde{\mathbf{z}}_l - \mathbf{H}_l \tilde{\mathbf{x}}) = -\mathbf{H}_0 (\mathbf{x}^{(m)} - \tilde{\mathbf{x}}), \quad m \geq 0.$$

This together with Theorem VII.2 implies that $\tilde{\mathbf{z}}_l^{(m)}$, $m \geq 1$, in the iterative algorithm (VII.9) and (VII.10) converges to $\tilde{\mathbf{z}}_l - \mathbf{H}_l \tilde{\mathbf{x}}$ exponentially, where $l = 0, 1$.

By (VII.12) and (VII.14) in Theorem VII.2, the iterative distributed algorithm (VII.9) and (VII.10) has fast convergence rate when a large radius parameter r is chosen. In that case, heavier burden arises at each iteration, which implies that each vertex in the graph \mathcal{G} should have more data storages, better computing abilities and stronger communication capacities in real world applications. Shown in Tables I and II are the average $E_{m,r}$ of $\|\mathbf{x}^{(m)} - \mathbf{x}\|_\infty / \|\mathbf{x}\|_\infty$ over 50 trials versus the number $m \geq 1$ of iterations and the radius parameter $r \geq 0$, where $(\mathbf{H}_{0,n}^{\text{spln}}, \mathbf{H}_{1,n}^{\text{spln}})$, $n = 1, 2$ are used as analysis filter banks, the signal \mathbf{x} in Tables I and II is randomly selected on the Minnesota traffic graph and on the random geometric graph RGG₄₀₉₆ in Figure 2 respectively. This demonstrates that the iterative distributed algorithm (VII.9) and (VII.10) converges faster for larger radius r , and the original signal can be well approximated in one step when a large radius r is chosen, see Tables I and II.

By (VII.12) and Theorem VII.2, there is a radius parameter r_0 such that the iterative distributed algorithm (VII.9) and (VII.10) converges exponentially whenever $r \geq r_0$. We can select the above radius parameter r_0 to be independent of the size of the graph \mathcal{G} . Our simulation indicates that the iterative distributed algorithm (VII.9) and (VII.10) with $r = 0$, i.e. the Jacobi iterative method by Remark VII.1, diverges for some bounded inputs on the Minnesota traffic graph and on some random geometric graphs, see the first column of Tables I and II.

TABLE I
PERFORMANCE OF THE ITERATIVE DISTRIBUTED RECONSTRUCTION ALGORITHM TO RECOVER SIGNALS ON THE MINNESOTA TRAFFIC GRAPH

$n = 1$						
$E_{m,r} \backslash r$	0	1	2	3	4	6
m						
1	.4155	.2220	.0375	.0160	.0033	.0003
2	.1355	.0238	.0007	.0001	.0000	.0000
3	.0547	.0039	.0000	.0000	.0000	.0000
4	.0226	.0006	.0000	.0000	.0000	.0000
5	.0098	.0000	.0000	.0000	.0000	.0000
10	.0002	.0000	.0000	.0000	.0000	.0000

$n = 2$						
$E_{m,r} \backslash r$	0	1	2	3	4	6
m						
1	1.1988	.6563	.3187	.1523	.0725	.0178
2	1.1662	.2315	.0518	.0136	.0029	.0002
3	1.4550	.1162	.0125	.0017	.0002	.0000
4	1.4697	.0567	.0026	.0002	.0000	.0000
5	2.5386	.0296	.0006	.0000	.0000	.0000
7	4.7083	.0082	.0000	.0000	.0000	.0000
10	12.7921	.0013	.0000	.0000	.0000	.0000
14	52.4168	.0001	.0000	.0000	.0000	.0000

TABLE II
PERFORMANCE OF THE ITERATIVE DISTRIBUTED RECONSTRUCTION ALGORITHM TO RECOVER SIGNALS ON THE RANDOM GEOMETRIC GRAPH RGG_{4096} IN FIGURE 2

$n = 1$						
$E_{m,r} \backslash r$	0	1	2	3	4	5
m						
1	.4182	.1301	.0156	.0035	.0006	.0001
2	.1963	.0083	.0002	.0000	.0000	.0000
3	.1143	.0008	.0000	.0000	.0000	.0000
4	.0699	.0000	.0000	.0000	.0000	.0000
10	.0050	.0000	.0000	.0000	.0000	.0000
19	.0001	.0000	.0000	.0000	.0000	.0000

$n = 2$						
$E_{m,r} \backslash r$	0	1	2	3	4	5
m						
1	1.5267	.4674	.1487	.0437	.0159	.0049
2	2.8586	.1098	.0120	.0011	.0001	.0000
3	6.6794	.0374	.0014	.0000	.0000	.0000
4	16.4089	.0121	.0002	.0000	.0000	.0000
5	40.9430	.0041	.0000	.0000	.0000	.0000
8	672.8632	.0002	.0000	.0000	.0000	.0000

VIII. DISTRIBUTED DENOISING

Given an NSGFB with analysis filter bank $(\mathbf{H}_0, \mathbf{H}_1)$ and synthesis filter bank $(\mathbf{G}_0, \mathbf{G}_1)$, we propose a denoising technique with hard thresholding operator T_τ applied to the high-pass subband signal, where $T_\tau(t) = \text{sgn}(t)(|t| - \tau)_+$ is the hard thresholding function with threshold value $\tau \geq 0$, cf. [26], [27], [45], [46]. Presented in Figure 5 is the block diagram of the proposed denoising procedure. In this section, we demonstrate the performance of the proposal denoising procedure associated with spline NSGFBs, which can be implemented in a distributed manner.

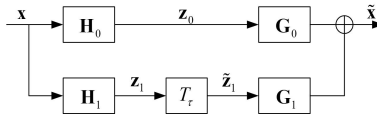


Fig. 5. Block diagram of the proposed denoising procedure, where \mathbf{x} is the noisy input and $\tilde{\mathbf{x}}$ is the denoised output.

TABLE III
DENOISING PERFORMANCE ON THE MINNESOTA TRAFFIC GRAPH MEASURED WITH THE STANDARD ℓ^2 -SNR

η	1/32	1/16	1/8	1/4	1/2	1
Input ℓ^2 -SNR	34.89	28.85	22.83	16.82	10.81	4.75
graphBior	34.43	28.91	24.06	18.21	12.79	7.39
OSGFB	38.25	32.59	24.44	16.70	12.54	4.69
PRT	35.31	29.41	23.74	18.46	15.45	12.77
NSGFB-B1	37.50	31.45	25.43	18.91	13.18	7.39
NSGFB-B2	37.25	30.74	24.95	18.53	13.32	7.68
NSGFB-L1	38.49	32.44	26.42	19.25	13.82	8.34
NSGFB-L2	37.25	30.67	24.91	18.16	13.33	7.88

In the simulations, the noisy input is

$$\mathbf{x} = \mathbf{x}_o + \boldsymbol{\epsilon}, \quad (\text{VIII.1})$$

where $\mathbf{x}_o = (x_{o,i})_{i \in V}$ is the original graph signal and the noise $\boldsymbol{\epsilon} = (\epsilon_i)_{i \in V}$ has value ϵ_i at vertex $i \in V$ randomly selected in the range $[-\eta, \eta]$. The spline NSGFBs have analysis spline filter banks ($\mathbf{H}_{0,n}^{\text{spln}}, \mathbf{H}_{1,n}^{\text{spln}}$) in (III.9) and synthesis spline filter banks being either ($\mathbf{G}_{0,n}^{\text{B,spln}}, \mathbf{G}_{1,n}^{\text{B,spln}}$) in (V.8) or ($\mathbf{G}_{0,n}^{\text{L,spln}}, \mathbf{G}_{1,n}^{\text{L,spln}}$) in (VI.9), where $n \geq 1$. They are abbreviated by NSGFB-B n and NSGFB-L n respectively. The denoising procedure is performed by retaining the low-pass subband signal $\mathbf{z}_0 = \mathbf{H}_{0,n}^{\text{spln}} \mathbf{x}$ and applying the hard thresholding operation T_τ to the high-pass subband signal $\mathbf{z}_1 = \mathbf{H}_{1,n}^{\text{spln}} \mathbf{x}$, where $\tau > 0$ is chosen appropriately. Thus the denoised output is

$$\tilde{\mathbf{x}} = \mathbf{G}_{0,n}^{\text{B,spln}} \mathbf{z}_0 + \mathbf{G}_{1,n}^{\text{B,spln}} T_\tau(\mathbf{z}_1)$$

for NSGFB-B n , and

$$\tilde{\mathbf{x}} = \mathbf{G}_{0,n}^{\text{L,spln}} \mathbf{z}_0 + \mathbf{G}_{1,n}^{\text{L,spln}} T_\tau(\mathbf{z}_1)$$

for NSGFB-L n respectively, where $n \geq 1$. For the above denoising procedure, we use $20 \log_{10} \|\mathbf{x}_o\|_p / \|\mathbf{x} - \mathbf{x}_o\|_p$ to measure the input ℓ^p -signal-to-noise ratio (ℓ^p -SNR) in dB, and $20 \log_{10} \|\mathbf{x}_o\|_p / \|\tilde{\mathbf{x}} - \mathbf{x}_o\|_p$ to measure the output ℓ^p -SNR in dB, where $1 \leq p \leq \infty$.

The Minnesota traffic graph is a test bed for various techniques in signal processing on graphs of medium size ([8], [20], [22], [26]). The denoising performance of the proposed spline NSGFBs on the Minnesota graph is presented in Table III, where the original signal \mathbf{x}_o is the blockwise constant function in Figure 3, the threshold value τ is selected to be 3η , and the input and output ℓ^2 -SNRs are the average values over 50 trials. Shown also in Table III are the performance comparison with the biorthogonal graph filter bank (graphBior) in [21], the M -channel oversampled graph filter bank (OSGFB) in [22], and the pyramid transform (PRT) in [26], where the corresponding output ℓ^2 -SNRs are calculated from the accompanying codes in these references. It indicates that the spline NSGFBs and the OSGFB outperform other two methods in the small noise scenario, the spline NSGFBs have the best performance in the moderate noise environment, and the PRT stands out from the rest in the strong noisy case.

Presented in Tables IV and V are the denoising performance of spline NSGFBs and the performance comparison with the graphBior in [21], the OSGFB in [22], and the PRT in [26] on the random geometric graph RGG_N , where $N = 4096$, the original signal \mathbf{x}_o is the blockwise polynomial in Figure 3, the threshold value τ is selected to be 3η , and the input and output ℓ^2 -SNRs in Table IV and the input and

TABLE IV
DENOISING PERFORMANCE ON THE RANDOM GEOMETRIC GRAPH RGG_{4096} MEASURED WITH THE STANDARD ℓ^2 -SNR

η	1/32	1/16	1/8	1/4	1/2	1
Input ℓ^2 -SNR	35.06	29.04	23.02	17.01	10.97	4.95
graphBior	33.82	28.61	23.27	18.20	13.21	8.34
OSGFB	31.69	26.37	20.79	16.40	13.40	11.13
PRT	32.89	27.51	22.44	17.70	14.21	11.81
NSGFB-B1	37.43	31.40	25.34	19.31	13.47	7.62
NSGFB-B2	36.65	30.63	24.89	19.37	13.80	8.25
NSGFB-L1	38.86	32.87	26.61	20.45	14.91	9.40
NSGFB-L2	36.08	29.97	24.27	19.16	13.92	9.05

TABLE V
DENOISING PERFORMANCE ON THE RANDOM GEOMETRIC GRAPH RGG_{4096} MEASURED WITH THE ℓ^∞ -SNR

η	1/32	1/16	1/8	1/4	1/2	1
Input ℓ^∞ -SNR	34.90	28.88	22.85	16.83	10.81	4.79
graphBior	23.45	17.28	11.12	5.34	0.32	-4.00
OSGFB	20.59	14.32	6.83	0.99	-1.99	-2.71
PRT	23.24	17.25	11.27	5.43	0.39	-2.15
NSGFB-B1	31.84	25.16	18.71	11.05	6.55	2.60
NSGFB-B2	26.86	20.34	14.67	8.32	3.55	1.67
NSGFB-L1	29.28	22.70	16.19	9.28	4.08	0.35
NSGFB-L2	24.66	17.91	12.27	6.72	0.48	-0.52

output ℓ^∞ -SNRs in Table V are the average values over 50 trials. It is observed that the spline NSGFBs proposed in this paper outperform the graphBior, OSBFB and PRT in small and moderate noise scenario, and that the spline NSGFBs have comparable performance with the rest in the strong noisy case. Also from Tables IV and V, we see that the differences between the input and output ℓ^p -SNRs for $p = 2, \infty$ are in some range. This confirms the conclusions in Proposition V.2 and Corollary VI.4 that the output noise is dominated by a multiple of the input noise.

Shown in Figure 6 is the input noise ϵ with $\eta = 1/16$ and differences between the original signal \mathbf{x}_o and the denoised signal $\tilde{\mathbf{x}}$ via the graphBior, OSGFB, PRT and spline NSGFBs, where a random geometric graph RGG_{4096} , original signal \mathbf{x}_o and noise ϵ are the same as in Tables IV and V. It indicates that all denoising techniques have satisfactory performance inside the same strip where the signal has small variation, and that the spline NSGFBs proposed in this paper achieve better performance visually on noise suppression than the other three methods do near the boundary of two adjacency strips where the signal has large variation.

The proposed NSGFBs can be implemented in a distributed manner and they are beneficial to (local) noise suppression on graphs of very large scale. Our simulations indicate that for random geometric graphs RGG_N with large size N and $1 \leq p \leq \infty$, the output ℓ^p -SNRs of spline NSGFBs have invisible change for the same input noise level when the graph size N increases.

APPENDIX

A. Proof of Proposition III.3

The first inequality follows from (III.7). Now we prove the second inequality. Write $\mathbf{A} = (a(i, j))_{i, j \in V}$, and define its Schur norm by

$$\|\mathbf{A}\|_S = \max \left(\sup_{i \in V} \sum_{j \in V} |a(i, j)|, \sup_{j \in V} \sum_{i \in V} |a(i, j)| \right).$$

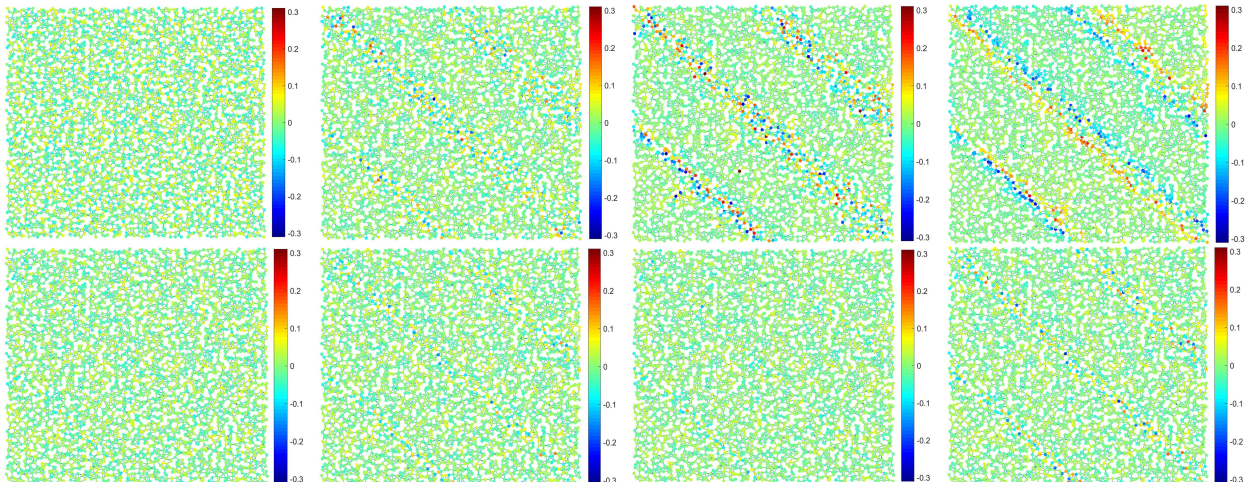


Fig. 6. Plotted on the top from left to right are the input noise ϵ , differences between the original signal \mathbf{x}_o and the denoised signal $\tilde{\mathbf{x}}$ obtained by the graphBior, OSGFB and PRT. Shown at the bottom from left to right are differences between the original signal \mathbf{x}_o and the denoised signal $\tilde{\mathbf{x}}$ obtained by NSGFB-B1, NSGFB-B2, NSGFB-L1 and NSGFB-L2.

It is well known that the filter bound $\|\mathbf{A}\|_{\mathcal{B}_p}$, $1 \leq p \leq \infty$, of a graph filter \mathbf{A} is dominated by its Schur norm,

$$\|\mathbf{A}\|_{\mathcal{B}_p} \leq \|\mathbf{A}\|_{\mathcal{S}} \text{ for all } 1 \leq p \leq \infty. \quad (\text{A.1})$$

Then it suffices to prove

$$\|\mathbf{A}\|_{\mathcal{S}} \leq D_1(\mathcal{G})(\sigma + 1)^d \|\mathbf{A}\|_{\infty}. \quad (\text{A.2})$$

For any $i \in V$, we obtain

$$\begin{aligned} \sum_{j \in V} |a(i, j)| &= \sum_{\rho(i, j) \leq \sigma} |a(i, j)| \leq \|\mathbf{A}\|_{\infty} \sum_{\rho(i, j) \leq \sigma} 1 \\ &\leq D_1(\mathcal{G})(\sigma + 1)^d \|\mathbf{A}\|_{\infty}, \end{aligned} \quad (\text{A.3})$$

where the second inequality follows from (II.2). Similarly for any $j \in V$, we have

$$\sum_{i \in V} |a(i, j)| \leq D_1(\mathcal{G})(\sigma + 1)^d \|\mathbf{A}\|_{\infty}. \quad (\text{A.4})$$

Combining (A.3) and (A.4) completes the proof.

B. Proof of Theorem IV.6

The upper bound estimate (IV.16) follows directly from Proposition III.3 and the observation that

$$\|\mathbf{H}_0\|_{\mathcal{B}_2} + \|\mathbf{H}_1\|_{\mathcal{B}_2} \leq 2\|\mathbf{H}\|_{\mathcal{B}_2}^{1/2}. \quad (\text{A.5})$$

Now we prove the lower bound estimate (IV.15). Set

$$\mathbf{B} = \mathbf{I} - \frac{\mathbf{H}}{\|\mathbf{H}\|_{\mathcal{B}_2}}. \quad (\text{A.6})$$

Then \mathbf{B} has bandwidth 2σ ,

$$\|\mathbf{B}\|_{\mathcal{B}_2} \leq (\kappa - 1)/\kappa, \quad (\text{A.7})$$

and

$$\mathbf{H}^{-1} = (\|\mathbf{H}\|_{\mathcal{B}_2})^{-1} \sum_{n=0}^{\infty} \mathbf{B}^n. \quad (\text{A.8})$$

Write $\mathbf{H}^{-1} = (g(i, j))_{i, j \in V}$. For $\kappa = 1$, we have

$$\mathbf{H}^{-1} = (\|\mathbf{H}\|_{\mathcal{B}_2})^{-1} \mathbf{I}. \quad (\text{A.9})$$

Now we consider the case that $\kappa > 1$. Set $\theta = \ln(\kappa/(\kappa - 1))$, and for $i, j \in V$ let $n_0(i, j)$ be the minimal integer such that $2n_0(i, j) \geq \rho(i, j)/\sigma$. Then

$$\begin{aligned} |g(i, j)| &\leq (\|\mathbf{H}\|_{\mathcal{B}_2})^{-1} \sum_{n=n_0(i, j)}^{\infty} \|\mathbf{B}^n\|_{\infty} \\ &\leq (\|\mathbf{H}\|_{\mathcal{B}_2})^{-1} \sum_{n=n_0(i, j)}^{\infty} \|\mathbf{B}\|_{\mathcal{B}_2}^n \\ &\leq (\|\mathbf{H}\|_{\mathcal{B}_2})^{-1} \kappa (1 - \kappa^{-1})^{n_0(i, j)} \\ &\leq \|\mathbf{H}^{-1}\|_{\mathcal{B}_2} \exp\left(-\frac{\theta}{2\sigma} \rho(i, j)\right), \end{aligned} \quad (\text{A.10})$$

where the first inequality follows from (A.8) and the observation that \mathbf{B}^n have bandwidth $2n\sigma$, the second one is true by (III.7), and the third one holds by (III.8) and (A.7).

From (A.9) we immediately get

$$\|\mathbf{H}^{-1}\|_{\mathcal{B}_p} = \|\mathbf{H}^{-1}\|_{\mathcal{B}_2} \quad (\text{A.11})$$

if $\kappa = 1$, and by (A.1) and (A.10), we have

$$\begin{aligned} \|\mathbf{H}^{-1}\|_{\mathcal{B}_p} &\leq \|\mathbf{H}^{-1}\|_{\mathcal{B}_2} \times \\ &\quad \sup_{i \in V} \sum_{n=0}^{\infty} \sum_{2n\sigma \leq \rho(i, j) < 2(n+1)\sigma} \exp\left(-\frac{\theta}{2\sigma} \rho(i, j)\right) \\ &\leq \|\mathbf{H}^{-1}\|_{\mathcal{B}_2} \sup_{i \in V} \sum_{n=0}^{\infty} e^{-n\theta} \mu\left(B(i, 2(n+1)\sigma - 1)\right) \\ &\leq (2\sigma)^d D_1(\mathcal{G}) \|\mathbf{H}^{-1}\|_{\mathcal{B}_2} \sum_{n=0}^{\infty} (n+1)^d (1 - \kappa^{-1})^n \\ &\leq (2\sigma)^d D_1(\mathcal{G}) \|\mathbf{H}^{-1}\|_{\mathcal{B}_2} \left(\left(\frac{1}{1-t}\right)^{(d)} \Big|_{t=1-\kappa^{-1}}\right) \\ &\leq d! (2\sigma)^d D_1(\mathcal{G}) \kappa^{d+1} \|\mathbf{H}^{-1}\|_{\mathcal{B}_2} \end{aligned} \quad (\text{A.12})$$

if $\kappa > 1$. Then

$$\begin{aligned} \|\mathbf{x}\|_p &\leq \|\mathbf{H}^{-1}\|_{\mathcal{B}_p} (\|\mathbf{H}_0^T\|_{\mathcal{B}_p} \|\mathbf{H}_0 \mathbf{x}\|_p + \|\mathbf{H}_1^T\|_{\mathcal{B}_p} \|\mathbf{H}_1 \mathbf{x}\|_p) \\ &\leq d! (2\sigma)^d D_1(\mathcal{G}) \kappa^{d+1} \|\mathbf{H}^{-1}\|_{\mathcal{B}_2} \\ &\quad \times (\|\mathbf{H}_0^T\|_{\mathcal{B}_p} \|\mathbf{H}_0 \mathbf{x}\|_p + \|\mathbf{H}_1^T\|_{\mathcal{B}_p} \|\mathbf{H}_1 \mathbf{x}\|_p) \\ &\leq d! 2^d (\sigma + 1)^{2d} (D_1(\mathcal{G}))^2 \kappa^{d+1} \|\mathbf{H}^{-1}\|_{\mathcal{B}_2} \\ &\quad \times (\|\mathbf{H}_0\|_{\mathcal{B}_2} \|\mathbf{H}_0 \mathbf{x}\|_p + \|\mathbf{H}_1\|_{\mathcal{B}_2} \|\mathbf{H}_1 \mathbf{x}\|_p) \\ &\leq d! 2^{d+1} (\sigma + 1)^{2d} (D_1(\mathcal{G}))^2 \kappa^{d+2} \|\mathbf{H}\|_{\mathcal{B}_2}^{-1/2} \\ &\quad \times \max(\|\mathbf{H}_0 \mathbf{x}\|_p, \|\mathbf{H}_1 \mathbf{x}\|_p), \\ &\leq d! 2^{d+1} (\sigma + 1)^{2d} (D_1(\mathcal{G}))^2 \kappa^{d+2} \|\mathbf{H}\|_{\mathcal{B}_2}^{-1/2} \\ &\quad \times (\|\mathbf{H}_0 \mathbf{x}\|_p^p + \|\mathbf{H}_1 \mathbf{x}\|_p^p)^{\frac{1}{p}}, \end{aligned} \quad (\text{A.13})$$

where the second inequality follows from (A.11) and (A.12), the third holds by Proposition III.3, and the fourth one is true by (A.5) and (IV.17). This proves (IV.15) and completes the proof.

C. Proof of Theorem V.1

By (III.3), (V.1), (V.2) and (V.3), we obtain

$$\begin{aligned} & \mathbf{G}_0 \mathbf{H}_0 + \mathbf{G}_1 \mathbf{H}_1 \\ &= Q_0(\mathbf{L}_{\mathcal{G}}^{\text{sym}}) P_0(\mathbf{L}_{\mathcal{G}}^{\text{sym}}) + Q_1(\mathbf{L}_{\mathcal{G}}^{\text{sym}}) Q_1(\mathbf{L}_{\mathcal{G}}^{\text{sym}}) \\ &= \mathbf{U}^T (Q_0(\mathbf{\Lambda}) P_0(\mathbf{\Lambda}) + Q_1(\mathbf{\Lambda}) P_1(\mathbf{\Lambda})) \mathbf{U} = \mathbf{U}^T \mathbf{U} = \mathbf{I}. \end{aligned}$$

This completes the proof.

D. Proof of Proposition V.2

Set $\mathbf{z}_0 = \mathbf{H}_0 \mathbf{x}$ and $\mathbf{z}_1 = \mathbf{H}_1 \mathbf{x}$. Then

$$\begin{aligned} \|\tilde{\mathbf{x}} - \mathbf{x}\|_p &\leq \|\mathbf{G}_0(\mathbf{z}_0 - \Psi_0(\mathbf{z}_0))\|_p + \|\mathbf{G}_1(\mathbf{z}_1 - \Psi_1(\mathbf{z}_1))\|_p \\ &\leq (\|\mathbf{G}_0\|_{\mathcal{B}_p} + \|\mathbf{G}_1\|_{\mathcal{B}_p}) \epsilon \\ &\leq D_1(\mathcal{G})(\tilde{\sigma} + 1)^d (\|\mathbf{G}_0\|_{\infty} + \|\mathbf{G}_1\|_{\infty}) \epsilon, \end{aligned} \tag{A.14}$$

where the first inequality follows from the perfect reconstruction condition (I.1) for the NSGFB constructed in Theorem V.1, the second one holds by (V.9), and the last estimate is true by Proposition III.3.

E. Proof of Theorem VI.1

By (VI.4) and (A.10), we have

$$\begin{aligned} |g_{l,L}(i, j)| &\leq \|\mathbf{H}^{-1}\|_{\mathcal{B}_2} \|\mathbf{H}_l\|_{\infty} \sum_{\rho(k,j) \leq \sigma} \exp\left(-\frac{\theta}{2\sigma} \rho(i, k)\right) \\ &\leq D_1(\mathcal{G}) \|\mathbf{H}^{-1}\|_{\mathcal{B}_2} \|\mathbf{H}_l\|_{\infty} (\sigma + 1)^d \\ &\quad \times \exp\left(-\frac{\theta}{2\sigma} \rho(i, j) + \frac{\theta}{2}\right), \quad i, j \in V, \end{aligned}$$

where $l = 0, 1$. This proves (VI.6).

F. Proof of Theorem VII.2

Set $\mathbf{y}^{(m)} = \tilde{\mathbf{x}} - \mathbf{x}^{(m)}$ and write $\mathbf{y}^{(m)} = (y^{(m)}(i))_{i \in V}$, $m \geq 0$. We claim that

$$\mathbf{y}^{(m)} = \mathbf{H}^{-1}(\mathbf{H}_0^T \tilde{\mathbf{z}}_0^{(m)} + \mathbf{H}_1^T \tilde{\mathbf{z}}_1^{(m)}), \quad m \geq 0. \tag{A.15}$$

The above claim holds for $m = 0$, since

$$\mathbf{y}^{(0)} = \tilde{\mathbf{x}} = \mathbf{H}^{-1}(\mathbf{H}_0^T \tilde{\mathbf{z}}_0 + \mathbf{H}_1^T \tilde{\mathbf{z}}_1) = \mathbf{H}^{-1}(\mathbf{H}_0^T \tilde{\mathbf{z}}_0^{(0)} + \mathbf{H}_1^T \tilde{\mathbf{z}}_1^{(0)})$$

by (VII.1) and (VII.10). Inductively for $m \geq 1$, we have

$$\begin{aligned} \mathbf{y}^{(m)} &= \mathbf{y}^{(m-1)} - \mathbf{v}^{(m)} \\ &= \mathbf{H}^{-1}(\mathbf{H}_0^T \tilde{\mathbf{z}}_0^{(m-1)} + \mathbf{H}_1^T \tilde{\mathbf{z}}_1^{(m-1)}) - \mathbf{v}^{(m)} \\ &= \mathbf{H}^{-1}(\mathbf{H}_0^T \tilde{\mathbf{z}}_0^{(m)} + \mathbf{H}_1^T \tilde{\mathbf{z}}_1^{(m)}) \end{aligned}$$

where the first and third equalities follow from (VII.9) and the second equality holds by the inductive hypothesis. This completes the proof of Claim A.15.

Write $(\chi_k^{2r} \mathbf{H} \chi_k^{2r})^{-1} = (g_k(i, j))_{i, j \in B(k, 2r)}$ and

$$\chi_k^r (\chi_k^{2r} \mathbf{H} \chi_k^{2r})^{-1} \chi_k^{2r} \mathbf{H} (\chi_k^{2r+2\sigma} - \chi_k^{2r}) = (\tilde{g}_k(i, j))_{i, j \in V}, \quad k \in V. \tag{A.16}$$

Following the argument used to prove (A.10), we have

$$|g_k(i, j)| \leq \|\mathbf{H}^{-1}\|_{\mathcal{B}_2} \exp\left(-\frac{\theta}{2\sigma}\rho(i, j)\right) \quad (\text{A.17})$$

for all $i, j \in B(k, 2r)$. By (III.7), (A.16) and (A.17), we obtain

$$\tilde{g}_k(i, j) = 0 \quad (\text{A.18})$$

where either $i \notin B(k, r)$ or $j \notin B(k, 2r + 2\sigma) \setminus B(k, 2r)$, and

$$\begin{aligned} |\tilde{g}_k(i, j)| &\leq \|\mathbf{H}^{-1}\|_{\mathcal{B}_2} \|\mathbf{H}\|_{\infty} \sum_{l \in B(j, 2\sigma)} \exp\left(-\frac{\theta}{2\sigma}\rho(i, l)\right) \\ &\leq D_1(\mathcal{G})(2\sigma + 1)^d \kappa \exp\left(-\frac{\theta}{2\sigma}r + \theta\right) \end{aligned} \quad (\text{A.19})$$

where $i \in B(k, r)$ and $j \in B(k, 2r + 2\sigma) \setminus B(k, 2r)$.

Write $\mathbf{v}_k^{(m)} = (v_k^{(m)}(i))_{i \in V}$, $m \geq 1$, $k \in V$. By (VII.9), (A.15), we have

$$\begin{aligned} \chi_k^r(\mathbf{v}_k^{(m)} - \mathbf{y}^{(m-1)}) &= \chi_k^r(\chi_k^{2r} \mathbf{H} \chi_k^{2r})^{-1} \chi_k^{2r} \\ &\quad \times \mathbf{H}(\chi_k^{2r+2\sigma} - \chi_k^{2r}) \mathbf{y}^{(m-1)}. \end{aligned}$$

Combining the above equation with (A.18) and (A.19), we get

$$\begin{aligned} |v_k^{(m)}(i) - y^{(m-1)}(i)| &= \left| \sum_{j \in B(k, 2r+2\sigma)} \tilde{g}_k(i, j) y^{(m-1)}(j) \right| \\ &\leq D_1(\mathcal{G})(2\sigma + 1)^d \kappa \exp\left(-\frac{\theta}{2\sigma}r + \theta\right) \\ &\quad \times \left(\sum_{j \in B(i, 3r+2\sigma)} |y^{(m-1)}(j)| \right), \quad i \in B(k, r). \end{aligned} \quad (\text{A.20})$$

This together with (VII.9) implies that

$$\begin{aligned} |y^{(m)}(i)| &= |v^{(m)}(i) - y^{(m-1)}(i)| \\ &\leq \frac{1}{\mu(B(i, r))} \sum_{k \in B(i, r)} |v_k^{(m)}(i) - y^{(m-1)}(i)| \\ &\leq D_1(\mathcal{G})(2\sigma + 1)^d \kappa \exp\left(-\frac{\theta}{2\sigma}r + \theta\right) \\ &\quad \times \left(\sum_{j \in B(i, 3r+2\sigma)} |y^{(m-1)}(j)| \right) \end{aligned} \quad (\text{A.21})$$

for all $i \in V$ and $m \geq 1$. Using the above componentwise estimate, we obtain

$$\|\mathbf{y}^{(m+1)}\|_p \leq \delta_{r, \sigma} \|\mathbf{y}^{(m)}\|_p, \quad m \geq 0. \quad (\text{A.22})$$

Iteratively applying the above estimate proves (VII.14).

REFERENCES

- [1] I. F. Akyildiz, W. Su, Y. Sankarasubramaniam, and E. Cayirci, "Wireless sensor networks: a survey," *Comput. Netw.*, vol. 38, pp. 393-422, Mar. 2002.
- [2] C. Chong and S. Kumar, "Sensor networks: evolution, opportunities, and challenges," *Proc. IEEE*, vol. 91, pp. 1247-1256, Aug. 2003.
- [3] J. Yick, B. Mukherjee, and D. Ghosal, "Wireless sensor network survey," *Comput. Netw.*, vol. 52, pp. 2292-2330, Aug. 2008.
- [4] R. Hebner, "The power grid in 2030," *IEEE Spectr.*, vol. 54, pp. 51-55, Apr. 2017.
- [5] C. Cheng, Y. Jiang, and Q. Sun, "Spatially distributed sampling and reconstruction," *Appl. Comput. Harmon. Anal.*, to be published.
- [6] F. Chung and L. Lu, *Complex Graphs and Networks* (CBMS Regional Conference Series in Mathematics 107), American Mathematical Society, 2006.
- [7] R. Coifman and M. Maggioni, "Diffusion Wavelets," *Appl. Comput. Harmon. Anal.*, vol. 26, pp. 53-94, July 2006.
- [8] D. I. Shuman, S. K. Narang, P. Frossard, A. Ortega, and P. Vandergheynst, "The emerging field of signal processing on graphs: Extending high-dimensional data analysis to networks and other irregular domains," *IEEE Signal Process. Mag.*, vol. 30, pp. 83-98, May 2013.
- [9] A. Sandryhaila and J. M. F. Moura, "Big data analysis with signal processing on graphs: Representation and processing of massive data sets with irregular structure," *IEEE Signal Process. Mag.*, vol. 31, pp. 80-90, Sept. 2014.
- [10] A. Sandryhaila and J. M. F. Moura, "Discrete signal processing on graphs," *IEEE Trans. Signal Process.*, vol. 61, pp. 1644-1656, Apr. 2013.
- [11] A. Sandryhaila and J. M. F. Moura, "Discrete signal processing on graphs: frequency analysis," *IEEE Trans. Signal Process.*, vol. 62, pp. 3042-3054, June 2014.
- [12] I. Daubechies, *Ten Lectures on Wavelets* (CBMS-NSF Regional Conference Series in Applied Mathematics 61), SIAM, 1992.
- [13] S. Mallat, *A wavelet tour of signal processing: the sparse way*, Academic Press, 2009.
- [14] M. Vetterli and J. Kovacevic, *Wavelets and Subband Coding*, Prentice Hall PTR, 1995.
- [15] M. Crovella and E. Kolaczyk, "Graph wavelets for spatial traffic analysis," in *Twenty-Second Annual Joint Conf. of the IEEE Computer and Communications (INFOCOM 2003)*, IEEE, vol. 3, San Francisco, USA, 2003, pp. 1848-1857.
- [16] M. Gavish, B. Nader, and R. R. Coifman, "Multiscale wavelets on trees, graphs and high dimensional data: Theory and applications to semi supervised learning," in *Proc. of the 27th Int. Conf. on Machine Learning*, Haifa, Israel, 2010, pp. 367-374.
- [17] G. Shen and A. Ortega, "Transform-based distributed data gathering," *IEEE Trans. Signal Process.*, vol. 58, pp. 3802-3815, July 2010.
- [18] W. Wang and K. Ramchandran, "Random multiresolution representations for arbitrary sensor network graphs," in *Proc. of 2006 IEEE Int. Conf. on Acoustics Speech and Signal Processing (ICASSP)*, IEEE, vol. 4, Toulouse, France, 2006, pp. 161-164.
- [19] D. K. Hammod, P. Vandergheynst, and R. Gribonval, "Wavelets on graphs via spectral graph theory," *Appl. Comput. Harmon. Anal.*, vol. 30, pp. 129-150, Mar. 2011.
- [20] S. K. Narang and A. Ortega, "Perfect reconstruction two-channel wavelet filter banks for graph structured data," *IEEE Trans. Signal Process.*, vol. 60, pp. 2786-2799, June 2012.
- [21] S. K. Narang and A. Ortega, "Compact support biorthogonal wavelet filterbanks for arbitrary undirected graphs," *IEEE Trans. Signal Process.*, vol. 61, pp. 4673-4685, Oct. 2013.
- [22] Y. Tanaka and A. Sakiyama, "M-Channel Oversampled Graph Filter Banks," *IEEE Trans. Signal Process.*, vol. 62, pp. 3578-3590, July 2014.
- [23] V. N. Ekambaram, G. C. Fanti, B. Ayazifar, and K. Ramchandran, "Spline-like wavelet filterbanks for multiresolution analysis of graph-structured data," *IEEE Trans. Signal Inf. Process. Netw.*, vol. 1, pp. 268-278, Dec. 2015.
- [24] R. M. Karp, "Reducibility among combinatorial problems," in *Complexity of Computer Computations*, R.E. Miller, J. W. Thatcher, J. D. Bohlinger, Ed., 1972, pp. 85-103.
- [25] H. Q. Nguyen, and M. N. Do, "Downsampling of signals on graphs via maximum spanning trees," *IEEE Trans. Signal Process.*, vol. 63, pp. 182-191, Jan. 2015.
- [26] D. I. Shuman, M. J. Faraji, and P. Vandergheynst, "A Multiscale Pyramid Transform for Graph Signals," *IEEE Trans. Signal Process.*, vol. 64, pp. 2119-2134, Apr. 2016.
- [27] N. Tremblay and P. Borgnat, "Subgraph-based filterbanks for graph signals," *IEEE Trans. Signal Process.*, vol. 64, pp. 3827-3840, Aug. 2016.
- [28] S. Chen, A. Sandryhaila, and J. Kovačević, "Distributed algorithm for graph signal inpainting," in *2015 IEEE Int. Conf. on Acoustics, Speech and Signal Processing (ICASSP)*, IEEE, Brisbane, Australia, 2015, pp. 3731-3735.
- [29] T. T. Doan and L. B. Carolyn, "Distributed primal dual methods for economic dispatch in power networks," *arXiv preprint, arXiv:1609.06287*, Sept. 2016.
- [30] D. Baker and A. Ephremides, "The architectural organization of a mobile radio network via a distributed algorithm," *IEEE Trans. on Commun.*, vol. 29, pp. 1694-1701, Nov. 1981.
- [31] K. Hwang and Z. Xu, "Scalable parallel computers for real-time signal processing," *IEEE Signal Process. Mag.*, vol. 13, pp. 50-66, July 1996.
- [32] Y. Vazquez and C. Malcolm, "Distributed multirobot exploration maintaining a mobile network," in *Proc. of Second IEEE Int. Conf. on Intelligent Systems*, IEEE, Varna, Bulgaria, 2004, pp. 113-118.
- [33] Q. Shi, H. Chen, H. Chen, and L. Jiang, "Distributed wireless sensor network localization via sequential greedy optimization algorithm," *IEEE Trans. Signal Process.*, vol. 58, pp. 3328-3340, June 2010.
- [34] Y. Zhang, T. Cao, S. Li, X. Tian, L. Yuan, H. Jia, and A. V. Vasilakos, "Parallel Processing Systems for Big Data: A Survey," *Proc. IEEE*, vol. 104, pp. 2114-2136, Nov. 2016.
- [35] Z. Wang and A. C. Bovik, "Mean squared error: love it or leave it?- A new look at signal fidelity measures," *IEEE Signal Processing Mag.*, vol. 98, pp. 98-117, Jan. 2009.
- [36] Q. Sun, "Localized nonlinear functional equations and two sampling problems in signal processing," *Adv. Comput. Math.*, vol. 40, pp. 415-458, Apr. 2014.

- [37] D. I. Shuman, B. Ricaud, and P. Vandergheynst, "Vertex-frequency analysis on graphs," *Appl. Comput. Harmon. Anal.*, vol. 40, pp. 260-291, Mar. 2016.
- [38] M. Penrose, *Random Geometric Graphs* (Oxford Studies in Probability 5), Oxford University Press, 2003.
- [39] M. S. Kotzagiannidis and P. L. Dragotti, "Sampling and Reconstruction of Sparse Signals on Circulant Graphs - An Introduction to Graph-FRI," *arXiv preprint, arXiv: 1606.08085*, June 2016.
- [40] A. Aldroubi, A. Baskakov, and I. Krishtal, "Slanted matrices, Banach frames, and sampling," *J. Funct. Anal.*, vol. 255, pp. 1667-1691, Oct. 2008.
- [41] C. E. Shin and Q. Sun, "Stability of localized operators," *J. Funct. Anal.*, vol. 256, pp. 2417-2439, Apr. 2009.
- [42] R. Tessera, "Left inverses of matrices with polynomial decay," *J. Funct. Anal.*, vol. 259, pp. 2793-2813, Dec. 2010.
- [43] Q. Sun, "Wiener's lemma for infinite matrices II," *Constr. Approx.*, vol. 34, pp. 209-235, Oct. 2011.
- [44] C. E. Shin and Q. Sun, "Polynomial control on stability, inversion and powers of matrices on simple graphs," *arXiv preprint, arXiv: 1705.07385*, May 2017.
- [45] A. Sakiyama and Y. Tanaka. "Oversampled graph Laplacian matrix for graph filter banks," *IEEE Trans. Signal Process.*, vol. 62, pp. 6425-6437, Dec. 2014.
- [46] A. Sakiyama, K. Watanabe, and Y. Tanaka, "Spectral graph wavelets and filter banks With low approximation error," *IEEE Trans. Signal Inf. Process. Netw.*, vol. 2, pp. 230-245, Sept. 2016.